Neuropharmacology 66 (2013) 274–289

Contents lists available at SciVerse ScienceDirect

Neuropharmacology

journal homepage: www.elsevier.com/locate/neuropharm

Neural substrates for the distinct effects of presynaptic group III metabotropic glutamate receptors on extinction of contextual fear conditioning in mice

Alice Dobi [a,1], Simone B. Sartori [b], Daniela Busti [c], Herman Van der Putten [d], Nicolas Singewald [b], Ryuichi Shigemoto [a,**], Francesco Ferraguti [c,*]

[a] Division of Cerebral Structure, National Institute for Physiological Sciences, Myodaiji, Okazaki 444-8787, Japan
[b] Department of Pharmacology and Toxicology, Center for Molecular Biosciences Innsbruck (CMBI), University of Innsbruck, Austria
[c] Department of Pharmacology, Innsbruck Medical University, Peter Mayr Strasse 1a, A-6020 Innsbruck, Austria
[d] Department of Neuroscience, Institutes for BioMedical Research, Novartis Pharma AG, Basel, Switzerland

ARTICLE INFO

Article history:
Received 15 February 2012
Received in revised form
9 May 2012
Accepted 17 May 2012

Keywords:
Amygdala
Intercalated cell
Prefrontal cortex
Tract tracing
Electron microscopy

ABSTRACT

The group III metabotropic glutamate (mGlu) receptors mGlu7 and mGlu8 are receiving increased attention as potential novel therapeutic targets for anxiety disorders. The effects mediated by these receptors appear to result from a complex interplay of facilitatory and inhibitory actions at different brain sites in the anxiety/fear circuits. To better understand the effect of mGlu7 and mGlu8 receptors on extinction of contextual fear and their critical sites of action in the fear networks, we focused on the amygdala. Direct injection into the basolateral complex of the amygdala of the mGlu7 receptor agonist AMN082 facilitated extinction, whereas the mGlu8 receptor agonist (S)-3,4-DCPG sustained freezing during the extinction acquisition trial. We also determined at the ultrastructural level the synaptic distribution of these receptors in the basal nucleus (BA) and intercalated cell clusters (ITCs) of the amygdala. Both areas are thought to exert key roles in fear extinction. We demonstrate that mGlu7 and mGlu8 receptors are located in different presynaptic terminals forming both asymmetric and symmetric synapses, and that they preferentially target neurons expressing mGlu1α receptors mostly located around ITCs. In addition we show that mGlu7 and mGlu8 receptors were segregated to different inputs to a significant extent. In particular, mGlu7a receptors were primarily onto glutamatergic afferents arising from the BA or midline thalamic nuclei, but not the medial prefrontal cortex (mPFC), as revealed by combined anterograde tracing and pre-embedding electron microscopy. On the other hand, mGlu8a showed a more restricted distribution in the BA and appeared absent from thalamic, mPFC and intrinsic inputs. This segregation of mGlu7 and mGlu8 receptors in different neuronal pathways of the fear circuit might explain the distinct effects on fear extinction training observed with mGlu7 and mGlu8 receptor agonists.

This article is part of a Special Issue entitled 'Metabotropic Glutamate Receptors'.

1. Introduction

Classical fear conditioning provides one of the most powerful models for studying the neural mechanisms of fear and pathological anxiety, both in animals and humans (Mahan and Ressler, 2012). During fear conditioning, associations are formed between an aversive stimulus and conditioned stimuli such as neutral environmental cues that are on the whole characteristic for that particular aversive situation. Re-exposure to the conditioned stimulus in absence of the predicted punishment eventually leads to fear extinction. Typically a fear response spontaneously recovers with the passage of time indicating that the original fear memory was not erased but complemented by a parallel inhibitory memory trace encoding the safety of the conditioned stimulus in that particular extinction context (Myers and Davis, 2007). Extinction of conditioned fear represents the basic paradigm of current exposure-based interventions in the therapy of human anxiety disorders (Phelps et al., 2004).

* Corresponding author. Tel.: +43 512 9003 71204; fax: +43 512 9003 72300.
** Corresponding author. Tel.: +81 564 595278; fax: +81 564 595275.
E-mail addresses: shigemot@nips.ac.jp (R. Shigemoto), Francesco.ferraguti@i-med.ac.at (F. Ferraguti).
[1] Current address: Section on Neuronal Structure (SNS), Laboratory for Integrative Neuroscience (LIN) NIAAA-NIH, 5625 Fishers Lane, Room TS-24, Bethesda, MD 20892-9411, USA.

0028-3908
doi:10.1016/j.neuropharm.2012.05.025

The formation of context-specific fear extinction is believed to involve a distributed neuronal network comprising the hippocampus, thalamus and ventromedial prefrontal cortex (mPFC) (Quirk and Mueller, 2008), which are strongly interconnected with the amygdaloid complex (Pitkänen, 2000). The role of the mPFC was proposed to ultimately control amygdala activity (Quirk and Beer, 2006). In fact, stimulation of the infralimbic component (IL) of the mPFC blocks the expression of conditioned fear, likely by altering inhibitory networks within the amygdala (Amano et al., 2010). Over the past decade evidence has accumulated pointing to a critical role of the basolateral complex of the amygdala (BLA) in the expression of contextual fear (Goosens and Maren, 2001; Muller et al., 1997) and in the acquisition of extinction (Herry et al., 2010). While enhanced activation of inhibitory circuits within the BLA may constrain the impact of sensory inputs at principal neurons, the intercalated cell clusters (ITCs) have been proposed to act as an inhibitory gate between the BLA and the central nucleus under cortical control, thus regulating amygdala output (Ehrlich et al., 2009; Pape and Pare, 2010). ITCs have emerged as a pivotal structure for inhibition of the expression of conditioned fear and for the storage of extinction memory (Likhtik et al., 2008). Although in recent years the cellular organization of the ITCs has been intensively investigated (Busti et al., 2011; Geracitano et al., 2007; Manko et al., 2011; Royer et al., 2000), many of the neural circuits and neurochemical systems involving the ITCs remain unclear.

Anatomical evidence has shown that group III metabotropic glutamate (mGlu) receptors are enriched in the amygdala and particularly in association with the ITCs (Masugi et al., 1999). Selective activation or blockade of these mGlu receptors was shown to alter anxiety and fear responses (Swanson et al., 2005). In particular, mGlu7-null mice showed a marked reduction in the acquisition of appetitive and aversive conditioning (Callaerts-Vegh et al., 2006; Masugi et al., 1999), as well as deficits in the extinction of conditioned emotional responses (Fendt et al., 2008; Goddyn et al., 2008). Measures of anxiety in mGlu8-deficient mice gave rise to inconsistent results (Duvoisin et al., 2005; Gerlai et al., 2002; Robbins et al., 2007). However, recent work revealed in these animals robust deficits in the expression of contextual conditioned fear and chlordiazepoxide-induced facilitation of extinction (Fendt et al., 2010).

Here, we investigated the potential influence of acute pharmacological activation of mGlu7 and mGlu8 receptors on extinction of contextual fear. In addition, we carried out a detailed characterization of the synaptic distribution of these receptors in the neural circuits within the amygdala likely implicated in the extinction of fear conditioning. Large neurons present at the border of ITC clusters and expressing the mGlu1α receptor (Busti et al., 2011) were also analyzed as possible preferential targets of inputs containing group III mGlu receptors.

2. Materials and methods

2.1. Animals

The reported studies were carried out on adult male C57Bl/6J mice (25–30 g). Before use, the animals were housed in groups of five under controlled laboratory conditions (12:12 h light/dark cycle with lights on at 07:00 h; 21 ± 1 °C; 60% humidity) with food and water *ad libitum* for at least two weeks after delivery from the supplier (Institut für Labortierkunde und –genetik, University of Vienna, Himberg, Austria or Japan SLC Inc., Hamamatsu, Japan). All experimental protocols were approved by the Austrian Animal Experimentation Ethics Board (GZ66.011/58-BrGT/2004 and GZ66.011/02-BrGT/2007) or by the National Institute for Physiological Science's Animal care and Use Committee in compliance with both the European Convention for the Protection of Vertebrate Animals used for Experimental and Other Scientific Purposes (ETS no. 123) and the European Communities Council Directive of 24 November 1986 (86/609/EEC). The authors further attest that all efforts were made to minimize animal suffering, the number of animals used, and to use alternatives to *in vivo* techniques whenever available.

2.2. Drug injections

Guide canulae (25 gauge, 11 mm in length), aimed to target the dorsal pole of the BLA [−1.2 mm caudal, 3.2 mm lateral and 4.0 mm ventral to Bregma according to the Franklin and Paxinos mouse brain atlas (2001)], were bilaterally implanted into the skull of anaesthetised mice ($n = 51$; 50 mg/kg i.p. sodium pentobarbital) and fixed with two stainless screws and dental cement. Seven days after surgery and 15 min before the onset of the behavioural experiments, the stylets of the guide canulae were replaced by injection microcanulae (31 gauge), which extended the guide canulae by 1 mm, thus, reaching the BLA. (S)-3,4-DCPG (Tocris, Bristol, UK) and AMN082 (synthesized internally at Novartis) were dissolved in artificial cerebrospinal fluid (aCSF). Mice were randomly assigned to 3 treatment groups, which were injected with either vehicle (aCSF), AMN082 (300 pmol) or (S)-3,4-DCPG (10 nmol) in a volume of 0.1 μl per side at a rate of 0.05 μl/min. The microcanulae were left in place for another 2 min.

2.3. Contextual fear conditioning

After surgery, mice were housed in groups of two to three until testing. They were handled once daily for three days and familiarised to the injection procedure. Behavioural experiments were performed between 09:00 and 16:00 h. Fear acquisition, extinction training and extinction recall were performed in two identical, brightly illuminated (300 lux) conditioning chambers (26 × 30 × 32 cm; Coulbourn Instruments, USA) with floors of stainless steel bars. The rods were connected to a shock source and grid scrambler (Coulbourn Instruments, USA) for delivery of the footshock used as unconditioned stimulus. The chambers were cleaned with water after each use. Video cameras were mounted above each chamber for recording of the animal's behaviour during the exposure to the context.

For fear acquisition, mice were placed into the conditioning chamber and five mild foot shocks (0.7 mA, 2 s) were delivered. A 2 min stimulus-free period preceded, separated and followed the unconditioned stimulus presentations. After 24 and 48 h, animals were replaced into the same chamber for 30 min of extinction training and 8 min of extinction recall in the absence of unconditioned stimulus presentations, respectively. Each testing session was continuously recorded and the freezing behaviour displayed by the mice was subsequently analyzed in 2 min bin intervals for fear acquisition, in 1 min bin intervals for fear extinction or for the total time interval for extinction recall, by an experienced observer blind to the treatment groups. The simultaneous display of a horizontal position of the head, rigid hunched position and stiffening/lifting of the tail by the mice was taken as freezing behaviour (Fanselow, 1980).

2.4. Locomotor activity in the conditioning chamber

Unconditioned mice were placed into the conditioning chamber and their spontaneous activity was recorded for 30 min by a video camera positioned above the chamber. The distance travelled was registered by a tracking system (VideoMot2, TSE Systems GmbH, Bad Homburg, Germany). In addition, the time each mouse spent in freezing behaviour was analyzed as described above.

Possible effects of (S)-3,4-DCPG on motor coordination were tested on the accelerating rotarod (TSE Systems GmbH, Bad Homburg, Germany) according to a previous protocol with slight modifications (Singewald et al., 2004). Mice were placed onto a slowly (4 rpm) rotating rod, which was then continuously accelerated to 40 rpm within 5 min. Mice were given an intense training (3 × 3 with a 5 min intertrial interval) on the first day and further training sessions (1 × 3/day) on the two following days. On day 4, mice were injected with either (S)-3,4-DCPG or aCSF and given two test trials 20 and 40 min later, which corresponded to time points 5 and 25 min spent in the conditioning chambers. The latency to fall off the rod was automatically recorded. The maximum time on the rotarod was set at 5 min.

2.5. Histology and perfusions for immunocytochemistry

At the end of each behavioural experiment, animals were killed by an overdose of pentobarbital and the exact injection sites were histologically established in 50 μm-thick brain sections stained with cresyl violet. Behavioural data were analyzed only from those animals that were injected at the correct target sites.

For immunocytochemical light and electron microscopy experiments, mice were deeply anesthetized by intraperitoneal injection of Thiopental (250 mg/kg, i.p.; Sandoz, Kundl, Austria) and perfused transcardially with phosphate buffered saline (PBS; 0.9% NaCl, pH 7.4) followed by ice-cold fixative made of 4% w/v paraformaldehyde and 15% v/v of a saturated solution of picric acid in phosphate buffer (PB; 0.1 M, pH 7.4) for 15 min. For electron microscopy experiments, glutaraldehyde was added to the fixative at a final dilution of 0.05% v/v just before the perfusion. Brains were immediately removed from the skull, washed in 0.1 M PB and sliced coronally in 40 (for light microscopy) or 50 μm (for electron microscopy) thick sections, unless otherwise specified, on a Leica VT1000S vibratome (Leica Microsystems, Vienna, Austria). Sections were stored in 0.1 M PB containing 0.05% NaN_3 at 6 °C until immunocytochemical experiments were performed.

2.6. Antibodies

For this study, 3 different polyclonal antibodies against mGlu1α have been used, two of them raised in rabbit and one in Guinea pig. One of the rabbit polyclonal antibodies against mGlu1α was raised to a bacterial fusion protein containing amino acid residues 859–1199 of rat mGlu1α (Shigemoto et al., 1997). Immunoblot results indicated that the antibodies do not react with other mGlu receptors or proteins (Shigemoto et al., 1997). The second rabbit polyclonal antibody against mGlu1α was raised against a synthetic peptide corresponding to the amino acids 1116–1130 of the rat mGlu1α sequence (Diasorin, Stillwater, MN). Immunolabelling for this antibody was completely abolished by pre-adsorption with synthetic rat mGlu1α (manufacturer's technical information) and in brain sections of mice lacking the mGlu1 receptor (Ferraguti et al., 2004). The Guinea pig polyclonal antibody against mGlu1α was kindly provided by Prof. M. Watanabe (Dept. Anatomy, Hokkaido University, Sapporo, Japan) and was raised against a fusion protein containing amino acid residues 945–1127 of mouse mGlu1α (Tanaka et al., 2000). Also for this antibody immunolabelling was completely abolished in brain sections of mice lacking the mGlu1 receptor (Ferraguti et al., 2004).

The rabbit polyclonal anti-mGlu7a antibody was raised against a bacterial fusion protein containing the amino acid residues 874–915 of rat mGlu7a (Shigemoto et al., 1996, 1997). Immunoblot results and tests in heterologous expression systems indicated that the antibody does not react with other mGlu receptors or proteins. No immunolabelling was obtained in the brain of mice deficient in mGlu7 protein (Sansig et al., 2001).

The guinea pig polyclonal anti-mGlu8a antibody was raised against a synthetic peptide corresponding to the last 23 amino acids of mouse mGlu8a (Kinoshita et al., 1996). Immunoblot analysis showed an immunoreactive band of the expected molecular weight, which disappeared after pre-adsorption of the antibody with the immunogenic peptide (Kinoshita et al., 1996). No immunolabelling was obtained in the brain of mice deficient in mGlu8 protein (Ferraguti et al., 2005).

Guinea pig antibodies to the vesicular γ-aminobutyric acid transporter (VGAT), vesicular glutamate transporters (VGluT) 1 and 2 were generous gifts from Prof. M. Watanabe (Hokkaido University).

Biotinylated goat anti-PHA-L was purchased from Vector laboratories (Burlingame, CA; Product No. BA-0224).

2.7. Immunofluorescence experiments

Immunofluorescent experiments were carried out according to previously published procedures (Ferraguti et al., 2004) using slices obtained from 4 mice. Briefly, free-floating sections were incubated in blocking solution, composed of 20% normal goat serum (NGS), 0.1% TritonX (TX), 0.9% NaCl in 50 mM Tris (pH 7.4) for 1 h at room temperature (RT) and then in primary antibodies (see Table 1 for complete listing and dilutions), in combination or alone, made up in TBS, 0.1% TX, and 1% NGS for approximately 48 h (6 °C). Subsequently, after extensive washes in TBS, sections were incubated overnight (6 °C) with a mixture of appropriate secondary antibodies (see Table 1). Sections were then washed and mounted onto gelatin-coated slides in Vectashield (Vector Laboratories, Burlingame, CA). To control for a possible cross-reactivity between IgGs in double and triple immunolabeling experiments, some sections were processed through the same immunocytochemical sequence, except that only one primary antibody was applied; but the full complement of secondary antibodies was maintained. In addition, the secondary antibodies utilized were highly pre-adsorbed to the IgGs of numerous species. Immunofluorescence was studied using a Zeiss AxioImager M1 microscope (Zeiss, Vienna, Austria) with epi-fluorescence illumination equipped with the following filter blocks: Cy2/Alexa488 (excitation filter band pass [BP] 480/40 nm; reflection short-pass filter 505 nm; emission filter BP 527/30 nm) and Cy3 (excitation filter BP 545/25 nm; reflection short-pass filter 570 nm; emission filter BP 605/70 nm). Images were displayed and analyzed by the Openlab software (version 5.5.0; Improvision). Images were acquired through an ORCA-ER CCD camera (Hamamatsu, Hamamatsu City, Japan). Brightness and contrast were adjusted for the whole frame with no part of the frame modified independently in any way.

2.8. PHA-L injections

For labelling of projections from the intralaminar thalamus and mPFC to the BLA and ITCs, as well as from BLA to ITCs, adult male mice ($n = 10$) were injected unilaterally with *Phaseolus vulgaris* leucoagglutinin (PHA-L) into these regions using previously published procedures (Gu and Simerly, 1997). Briefly, animals were anesthetized with 7% chloral hydrate in 0.9% NaCl (0.5 ml/100 g body weight). A 2.5% solution of PHA-L (Vector) in 0.1 M sodium phosphate buffer (pH 7.8) was delivered iontophoretically into the posterior amygdala (Bregma −1.6, +3.3 ML, −5.1 DV), intralaminar thalamus (Bregma −1.0, 0 ML, −3.9 DV) or IL-mPFC (Bregma +2.0, +0.2 ML, −2.5 DV) through a stereotaxically positioned glass micropipette (tip diameter 15–20 μm), by applying a positive current (3.5–5 μA, 7 s on/off intervals) for 10–30 min. After 5–14 day survival period, mice were deeply anesthetized with sodium pentobarbital (50 mg/kg, i.p.) and perfused transcardially as described in 2.5. Serial coronal sections (50 μm thick), from injection sites to projection sites, were cut with a vibratome (Leica, Vienna, Austria). Every fifth section was used for immunocytochemical detection of PHA-L for light microscopy. Sections were first incubated in blocking buffer composed of 2% NGS in PBS for 1 h and then overnight at RT with 5 μg/ml biotinylated anti-PHA-L (Vector) in PBS containing 0.3% TX and 1% NGS. After extensive washes, the sections were incubated in the ABC complex (1:100, Vector) made up in PBS containing 0.1% TX for 2 h followed by diaminobenzidine (DAB) (0.5 mg/ml) and 0.003% H_2O_2, as the electron donor, for 5–6 min. If the injection sites were correctly placed and projection sites were strongly labelled, amygdala sections from these animals were processed for pre-embedding electron microscopy.

2.9. Pre-embedding immunocytochemistry for electron microscopy

Pre-embedding immunocytochemistry experiments were carried out according to previously published procedures (Sreepathi and Ferraguti, 2012). Briefly, free-floating sections were washed three times in 0.1 M PB, cryoprotected in 20% sucrose made in 0.1 M PB overnight at 6 °C. After removal of the sucrose, the sections were freeze-thawed twice to allow antibody penetration and then incubated in 20% NGS in TBS for 2 h at RT. After blocking, sections were exposed for ~72 h at 6 °C to primary antibodies (see Table 1) made up in a solution containing 2% NGS in TBS. After three washes in TBS, sections were incubated overnight at 6 °C with the appropriate secondary antibodies (Table 1). When a single primary antibody was used, it was visualized either by horseradish peroxidase (HRP) or by nanogold-silver-enhanced reaction. When more than one primary antibody was used, one of

Table 1
List of the concentrations and combinations of primary and secondary antibodies.

Primary antibody	Antigen/source	Species	Dilution	Secondary antibody	Dilution	Combinations
mGlu1α	Bacterial fusion protein (aa 859–1199, rat sequence)	Rabbit serum	1.0 μg/ml EM	Gt anti-Rb nanogold (Nanoprobes)	1:100	D, E, F, G
mGlu1α	Synthetic peptide (aa 1116–1130, rat sequence)	Rabbit IgG	1.0 μg/ml LM	Dnk anti-Rb Alexa488 (Invitrogen)	1:1000	d
mGlu1α	Fusion protein (aa 945–1127, mouse sequence)	G. Pig IgG	1.0 μg/ml LM	Dnk anti-G. Pig Alexa488 (Invitrogen)	1:1000	c
			EM	Gt anti-G. Pig nanogold (Nanoprobes)	1:100	H, I
				Gt anti-G. Pig Biotinylated (Vector)	1:100	C
mGlu8a	Synthetic peptide corresponding to the last 23 amino acids of the C-terminus of the mouse mGlu8a	G. Pig IgG	1.0 μg/ml LM	Dnk anti-G. Pig Cy3 (Jackson)	1:400	b, d
				Dnk anti-G. Pig Alexa488 (Invitrogen)	1:1000	e
			EM	Gt anti-G. Pig nanogold (Nanoprobes)	1:100	B, H
mGlu7a	Bacterial fusion protein (aa 874–915)	Rabbit IgG	1.0 μg/ml LM	Dnk anti-Rb Cy3 (Jackson)	1:400	a, c, e
			EM	Gt anti-Rb Biotinylated (Vector)	1:500	I
				Gt anti-Rb nanogold (Nanoprobes)	1:100	A, C, D, E, F, G
PHA-L	Vector	G. Pig IgG	5.0 μg/ml EM	Gt anti-G. Pig Biotinylated (Vector)	1:100	G, H
VGAT	Fusion protein (aa 31–112, mouse sequence)	G. Pig IgG	1.0 μg/ml EM	Gt anti-G. Pig Biotinylated (Vector)	1:100	F
VGluT1	Fusion protein (aa 511–560, rat sequence)	G. pig IgG	1.0 μg/ml EM	Gt anti-G. Pig Biotinylated (Vector)	1:100	D
VGluT2	Fusion protein (aa 519–582, rat sequence)	G. pig IgG	1.0 μg/ml EM	Gt anti-G. Pig Biotinylated (Vector)	1:100	E

Capital letters indicate reactions for pre-embedding electron microscopy, whereas small letters indicate reactions for immunofluorescence.
Abbreviations: Dnk, donkey; G. Pig, Guinea pig; Gt, goat, Rb, rabbit.

them was visualized by nanogold-silver-enhanced reaction and the second was visualized by HRP reaction. Silver enhancement was always carried out first. After several washes with TBS, sections incubated with Fab fragment secondary antibodies coupled to nanogold (1.4 nm) were extensively washed in milliQ water, followed by silver enhancement of the gold particles with the HQ kit (Nanoprobes Inc., Stony Brook, NY, USA) for ~5–10 min. Sections were then washed extensively in milliQ water and then with TB. Sections processed for the HRP reaction were incubated in ABC complex (diluted 1:100; Vector) made up in TB either overnight at 6 °C or at RT for 2 h and then washed in TB several times before the antigen/antibody complex was visualized by means of the DAB-H_2O_2 reaction. Sections were subsequently washed with 0.1 M PB and treated with 2% OsO_4 in 0.1 M PB for 30 min at RT. After several washes with 0.1 M PB and then with milliQ water, sections were contrasted with 1% uranyl-acetate in 50% ethanol for 30 min at RT, making sure they were protected from light. Sections were washed with milliQ water followed by graded ethanol and propylene oxide at RT. Sections were then quickly transferred into weighting boats containing epoxy resin (Durcupan ACM-Fluka, Sigma, Gillingham, UK) and kept overnight at RT. The following day, the sections were transferred onto siliconized slides, coverslipped with ACLAR® – film coverslips (Ted Pella, Inc., Redding, CA), and incubated for 3 days at 60 °C. Blocks containing specific nuclei of the amygdala were cut under a stereomicroscope and re-embedded in epoxy resin. Ultrathin sections (70 nm) were cut using a diamond knife (Diatome, Biel, Switzerland) on an ultramicrotome (Ultracut, Leica, Vienna, Austria), collected on copper slot grids coated with pioloform (Agar, Stansted, England) and analyzed with a transmission electron microscope (Jeol JEM-1010 or Philips CM120).

2.10. Statistical analysis

Behavioural data are presented as mean ± s.e.m. during 1, 2 and 5 min time periods in contextual fear conditioning and locomotor activity studies, respectively. Absolute freezing times were transformed into percentage scores. Statistical analysis of behavioural data was carried out by one-way ANOVA or two-way ANOVA with repeated measures followed by a Fisher's LSD test after a significant omnibus value. *P*-levels <0.05 were considered statistically significant, while $P < 0.08$ was used to indicate a trend towards significance.

To determine the sample size required for establishing the lack of group III mGlus in specific inputs we used prospectively Power analysis. Sample size was obtained by testing for one proportion using the software Java Applets for Power and Sample Size (Lenth, 2006-9). We assumed the frequency of PHA-L positive axon terminals labelled for presynaptic mGlu receptors to be 20% and a presumed lack of or occasional presence of receptors in these terminals to be 1%. We set the power to 0.90 and the alpha to 0.05; using these parameters Power analysis indicated a minimal sample size (number of synapses to be analyzed) of 23.

To estimate whether the type of target and of synapse formed by mGlu7 and mGlu8-containing terminals was different, the relative proportions were analyzed with the χ^2 test using the GraphPad Prism software (version 5.0c; GraphPad Software Inc., La Jolla, CA, USA).

3. Results

3.1. Effect of (S)-3,4-DCPG and AMN082 on extinction of learned contextual fear

In order to confine the pharmacological activity of the mGlu7 receptor agonist AMN082 and mGlu8 receptor agonist (S)-3,4-DCPG to amygdala networks, mice were bilaterally implanted with microcanulae targeting the BLA (Fig. 1A). Seven days after surgery, mice were subjected to contextual fear conditioning. Mice exhibited no freezing behaviour in the context prior to the presentation of the first footshock (first 2 min). Freezing levels constantly increased during conditioning to reach a maximum of approximately 40% (Fig. 1B). The maximum freezing level did not differ among experimental groups (time effect: $F_{5,150} = 64.106$, $P < 0.001$; treatment effect: $F_{2,30} = 1.076$, $P = 0.354$) (Fig. 1B). Twenty-four hours later, mice were randomly assigned to one of the 3 treatment groups and received microinjections of either

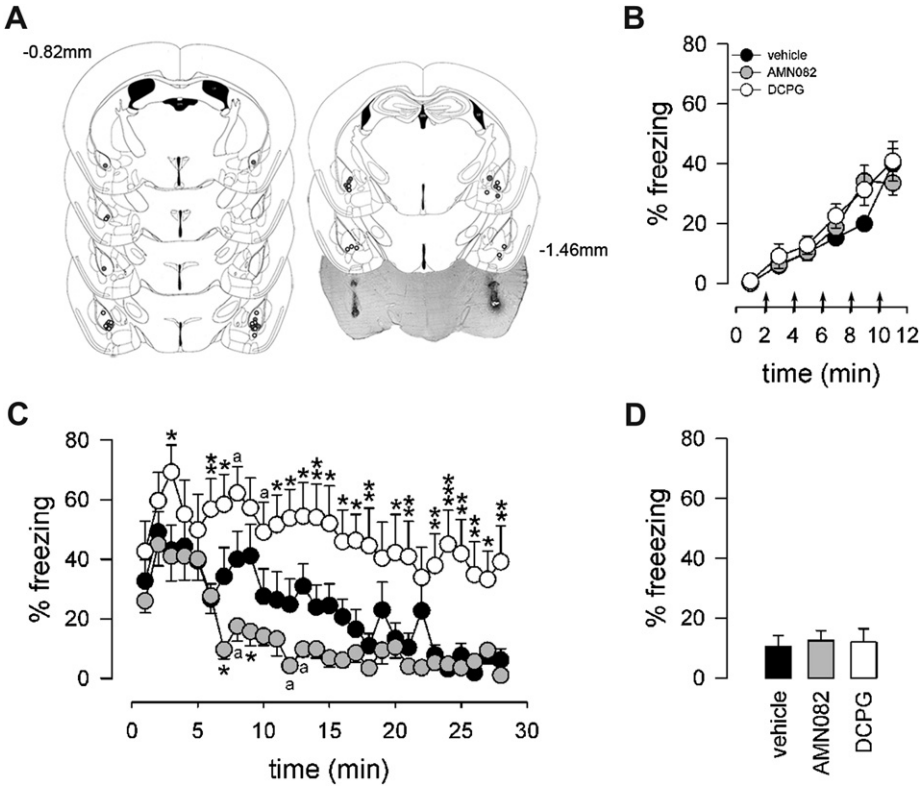

Fig. 1. Effect of intra-BLA injection of AMN082 (grey circles) or (S)-3,4-DCPG (white circles) on context-specific fear expression during fear conditioning, fear memory extinction and extinction recall. (A) Localisations of bilateral injection sites for AMN082 and (S)-3,4-DCPG in the BLA are shown in sequential coronal drawings (from Bregma −0.82 to −1.46 mm)(Paxinos and Franklin, 2001) and in a representative photomicrograph. (B) During contextual fear conditioning animals of all 3 experimental groups displayed increasing freezing responses to the context (arrows indicate delivery of foot shocks). (C) Intra-BLA injection of AMN082 facilitated the attenuation of freezing during extinction training, whereas (S)-3,4-DCPG inhibited it. (D) In the recall test no differences in fear expression to the conditioning context between vehicle-, (S)-3,4-DCPG- and AMN082-treated mice were observed. $N = 10–11$ per experimental group. $^{a}P < 0.08$, $^{*}P < 0.05$, $^{**}P < 0.01$, $^{**}P < 0.001$ drug-treated versus. vehicle-treated animals.

vehicle (aCSF), AMN082 or (S)-3,4-DCPG 15 min prior to the extinction trial. A significant treatment effect ($F_{2,29} = 8.028$, $P = 0.002$), time effect ($F_{29,841} = 12.513$, $P < 0.001$) and treatment × time interaction ($F_{58,841} = 1.720$, $P < 0.001$) was observed on extinction of contextual fear conditioning. In the conditioning context the initial freezing levels were similar in all 3 experimental groups (Fig. 1C). Freezing levels displayed by vehicle-treated mice were consistently decreased after 10 min of context exposure ($P = 0.004$ versus 2 min) reaching less than 15% freezing after 20 min of context exposure (Fig. 1C). The mGlu7 agonist AMN082 accelerated the decline in freezing levels as their percentage of freezing was significantly attenuated already after 6 min of context exposure ($P = 0.017$ versus 2 min) with an almost full extinction after 12 min (Fig. 1C). In contrast, in mice injected with (S)-3,4-DCPG freezing levels increased up to 70% within the first 3 min of context exposure ($P < 0.001$ versus 1 min) and stayed high for another 15 min (Fig. 1C). After this time point, mice began to show some reduction in freezing behaviour ($P = 0.036$ versus 2 min) that, however, was incomplete and remained relative high (~40%) till the end of the trial (Fig. 1C). Compared with control animals, (S)-3,4-DCPG-injected mice displayed elevated fear responses during most of the time of the extinction trial (Fig. 1C). At retest, 24 h later, mice from all three experimental groups did not differ in freezing levels displayed upon exposure to the conditioning chamber ($F_{2,27} = 0.070$, $P = 0.933$; Fig. 1D).

3.2. Effect of (S)-3,4-DCPG on motor performance

In order to exclude that the impaired extinction observed after (S)-3,4-DCPG-administration could be due to an effect of the drug on motor performance, we assessed the mice on the accelerating rotarod. Animals bilaterally implanted with canulae improved their motor performance over 15 training trials (data not shown). (S)-3,4-DCPG- and vehicle-treated mice did not differ in the latency to fall off the rod during the test trial at 20 min ($p = 0.916$) and at 40 min after microinjections (treatment effect: $F_{1,8} = 0.011$, $P = 0.920$; time effect: $F_{1,8} = 4.546$, $P = 0.066$; treatment × time interaction: $F_{1,8} = 0.018$, $P = 0.898$) (Fig. 2A). These results indicate no general motor-impairing properties produced by intra-BLA application of (S)-3,4-DCPG. We then studied the spontaneous locomotor activity in the conditioning chamber. Although mobility scores, as indicated by the distance travelled in the testing chamber, showed a clear tendency to be reduced in (S)-3,4-DCPG-treated mice as compared with vehicle-treated controls, no statistically significant treatment effect ($F_{1,8} = 3.898$, $P = 0.084$) or treatment × time interaction ($F_{5,40} = 2.312$, $P = 0.062$; Fig. 2B) was observed. In contrast, vehicle- and (S)-3,4-DCPG-treated animals differed in their freezing behaviour elicited by exposure to a novel context (treatment effect: $F_{1,8} = 7.901$, $P = 0.023$; time effect: $F_{5,40} = 8.141$, $P < 0.001$; treatment × time interaction: $F_{5,40} = 6.219$, $P < 0.001$). While vehicle-treated animals showed no freezing responses to the conditioning context, (S)-3,4-DCPG induced *per se* high levels of freezing, which declined over time and was absent after 20 min spent in the conditioning chamber (Fig. 2C).

3.3. Cellular and subcellular distribution of mGlu7a and mGlu8a in the mouse amygdala

To elucidate the molecular and cellular underpinnings of the behavioural effects of mGlu7 and mGlu8 receptor agonists injected intra-amygdala, we have then investigated at both light and electron microscopic level the cellular and subcellular distribution of these receptors using highly specific antibodies. We limited our analysis to the most abundant splice variants, namely mGlu7a and mGlu8a (Corti et al., 1998). However, this should not represent a limitation as the main splice variants for these receptors are generally coexpressed in the same brain regions (Corti et al., 1998; Ferraguti et al., 2005). Immunostaining for mGlu7a receptors appeared punctate, suggestive of a presynaptic location, and to decorate the soma and dendrites of principal cells and interneurons in the BLA as well as large neurons present at the outer border between the BLA and ITC clusters (Fig. 3A–B). Similarly, mGlu8a receptor labelling was particularly intense in boutons apposed to the dendrites of these large neurons (Fig. 4). In the basal nucleus of the amygdala (BA), mGlu7a immunoreactivity was much more prevalent than mGlu8a, being most likely present in terminals of local axon collaterals of pyramidal neurons. Double immunofluorescence experiments allowed us to identify the large neurons as containing mGlu1α receptors (Fig. 3B–I), which correspond to previously described large ITC neurons (Busti et al., 2011). The presynaptic location of mGlu7a and mGlu8a receptors was then established both in the BA and ITC by means of silver-intensified immunogold pre-embedding electron microscopy. For both receptors the labelling was restricted to the active zone of presynaptic axon terminals (Figs. 3J, 4J–K), which formed either asymmetric synapses on spines and dendrites or symmetric synapses on dendrites and somata. The type and frequency of synapses onto specific targets (namely spines, dendritic shafts or somata) was then analyzed in both the BA and ITCs. In the BA, 68% of the randomly-selected synapses ($n = 82$) containing presynaptic mGlu7a receptors were on spines, and of the remaining synapses, that were mostly present on dendrites, 62% were asymmetric. In the ITCs, mGlu7a positive terminals ($n = 43$) targeted spines in only 28% of the cases, and of the synapses on dendritic shafts 71% were asymmetric. The axon terminals containing mGlu8a receptors in the BA ($n = 41$) made mostly (56%) synaptic contacts with dendritic shafts, 30% of which formed asymmetric synapses, whereas the remaining synapses were on spines. In the ITC, only 21% of the

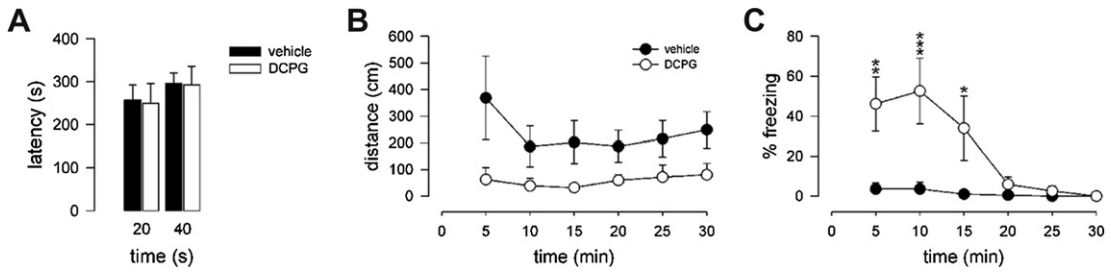

Fig. 2. Effect of intra-BLA injection of (S)-3,4-DCPG on locomotion. (A) (S)-3,4-DCPG did not influence motor coordination as indicated by the latency to fall off the rod when given either 20 or 40 min before the accelerating rotarod test. (B) Although spontaneous locomotor activity (assessed in 5 min time bins) in the conditioning chambers seemed to be reduced in (S)-3,4-DCPG-treated mice as compared with vehicle-treated controls, it did not reach statistical significance. (C) Intra-BLA injection of (S)-3,4-DCPG increased the percentage of freezing time as compared with vehicle-treatment. $N = 5$ per experimental group. $^{*}P < 0.05$, $^{**}P < 0.01$, $^{**}P < 0.001$ (S)-3,4-DCPG- versus. vehicle-treated animals.

analyzed synapses ($n = 95$) having axon terminals immunolabelled for the mGlu8a receptor were on spines, similar to what observed for mGlu7a positive inputs, and 61% of the mGlu8a-containing synapses on dendrites were asymmetric. We could, therefore, observe a significant difference in the BA ($P < 0.001$, χ^2 test) in the pattern of target innervation between mGlu7a and mGlu8a receptor-containing axon terminals, whereas in ITCs no differences were detected ($P = 0.22$, χ^2 test). These data suggest that in the BA these two mGlu receptors may be to a large degree segregated in independent afferents, whereas in the ITCs they could at least in part coexist.

In order to understand whether mGlu7a and mGlu8a receptors indeed coexist in the same presynaptic axon terminals targeting large ITC neurons, we performed double immunofluorescent experiments, which revealed a complex pattern of coexpression as some labelled boutons showed coexistence between mGlu7a and mGlu8a receptors whereas others appeared only labelled for mGlu7a or mGlu8a receptors, respectively (Fig. 5).

To assess whether the synapses on large mGlu1α+ ITC neurons and containing mGlu7a receptors in the presynaptic bouton were glutamatergic or GABAergic, we carried out triple-immunopre-embedding electron microscopy experiments. We used silver-intensified immunogold reactions for detecting presynaptic mGlu7a and postsynaptic mGlu1α receptors and immunoperoxidase for visualizing VGluT1, VGluT2 or VGAT. Immunoreactivity for mGlu7a was observed in GABAergic VGAT+ inputs as well as in both VGluT1 and VGluT2 glutamatergic afferents (Fig. 6). This indicates the presence of mGlu7a receptors in afferents originated from thalamic/hypothalamic areas as well as from the neocortex/hippocampus and/or BLA.

3.4. mPFC projections to the amygdala lack presynaptic mGlu7a and mGlu8a receptors

To identify the origin of the glutamatergic inputs containing mGlu7a and mGlu8a receptors, we carried out tracing experiments injecting iontophoretically in mice the sensitive anterograde tracer PHA-L combined with pre-embedding immuno-electron microscopy for revealing the presence of mGlu7a or mGlu8a receptors in the projections to the amygdala.

Because the mPFC plays a critical role in the expression and consolidation of fear extinction (Quirk and Mueller, 2008), we have injected PHA-L into the mPFC. To our knowledge, no tracing studies describing the projection from the mPFC to the amygdala in the brain of any mouse strain have been published. We show here two cases, selected from a larger series of injections, in which the injection site was mostly confined to the IL-PFC (Fig. 7A). However, as a few labelled neurons could be observed in the prelimbic component of the mPFC, we will refer here our tracing as originating from the mPFC. Similar to the rat (McDonald et al., 1996; Vertes, 2004), most of the fibres appeared to reach the amygdala through the medial forebrain bundle and then turning laterally through the substantia innominata. Some fibres were also observed running along the external capsule. Projections from the mPFC terminated mostly in the intermediate division of the BA, although some labelled boutons could be observed in ITC clusters placed along the intermediate capsule (Fig. 7B). Other portions of the amygdala such as the bed nucleus of the stria terminalis intra-amygdala, the medial nucleus and some of the superficial nuclei received also a relatively dense projection. Outside the amygdala, dense terminal and non-terminal projections were observed in the substantia innominata, nucleus accumbens, endopiriform nucleus, mediodorsal thalamus and lateral hypothalamus.

By means of combined anterograde tracing and pre-embedding immuno-electron microscopic methods, we have analyzed whether mPFC terminals forming synapses onto BA and ITC neurons possessed presynaptic mGlu7a or mGlu8a receptors, and second whether terminals containing group III mGlu receptors formed synapses with mGlu1α-expressing neurons in these areas. mPFC terminals formed only asymmetric synapses most of which (~95% in the BA; ~98% in the ITC) with dendritic spines and the remaining with dendritic shafts. As shown in Table 2, none of the terminals immunolabeled for PHA-L showed immunoreactivity for mGlu7a or mGlu8a receptors, suggesting that mPFC projections to the ITC or BA do not contain these group III presynaptic mGlu receptors (Fig. 7E and F).

3.5. Thalamic midline efferents to the amygdala contain presynaptic mGlu7a, but not mGlu8a receptors

Similar to the mPFC, also for the thalamic output to the amygdala no studies are available for the mouse brain. As thalamo-amygdala projections in the rat originate largely from midline nuclei (Ottersen and Ben-Ari, 1979; Su and Bentivoglio, 1990; Turner and Herkenham, 1991), we have injected PHA-L into the dorsal subdivision of the thalamic midline. The two cases presented here, selected from a larger series, showed little variability in the pattern of terminal labelling, therefore the descriptions below are representative for both animals. As shown in Fig. 8A, the tracer injections involved mainly the paraventricular, intermediodorsal and central medial nuclei. Labelled axons leaving the injection site projected laterally to the inferior thalamic peduncles and entered the amygdala from its rostral pole. The amygdaloid terminal zone was particularly intense in the intermediate division of the BA, moderate in the capsular and lateral divisions of the CE and weak in the medial division of the CE (Fig. 8B). A few labelled axons were also observed in the intermediate capsule and main nucleus of the ITC (Fig. 8C). Outside the amygdala intense innervation was observed in the dorso-medial striatum and moderate in the ventral pallidum, accumbens, claustrum–endopiriform nucleus and cingulate cortex.

A combined anterograde tracing and pre-embedding immuno-electron microscopy approach was carried out also for PHA-L labelled thalamic terminals. Thalamic terminals formed only asymmetric synapses most of which (~90% in the BA; ~95% in the ITC) with dendritic spines, whereas the remaining were on dendritic shafts. As shown in Table 2, approximately 23% of thalamic PHA-L labelled terminals on spines in the ITC possessed mGlu7a receptors presynaptically, 29% of which formed synapses with mGlu1α immunopositive profiles. In the BA, 33% of thalamic terminals with presynaptic mGlu7a receptors contacting dendrites and 8% contacting spines were made with mGlu1α-labelled neurons. Conversely, none of the terminals immunolabelled for PHA-L showed immunoreactivity for mGlu8a receptors, suggesting that also thalamic projections to the ITC or BA do not contain presynaptic mGlu8 receptors (Table 2; Fig. 8).

3.6. Intrinsic projections of the BA possess mGlu7a but not mGlu8a receptors

To investigate whether intrinsic projections from the BA possess group III mGlus and target ITC neurons, we injected PHA-L iontophoretically in the posterior parvicellular division of the BA (Fig. 9). In the two cases presented here, the terminal zone of labelled axons was most intense within the entire extent of the BA (Fig. 9C). Several neurons were found intensely labelled for PHA-L also in rostral areas of the BA and in the LA, possibly due to retrograde transport of the tracer. A robust projection was observed in the medial CEA whereas the innervation of the ITC seemed moderate to weak and mostly confined to the medial paracapsular cluster and

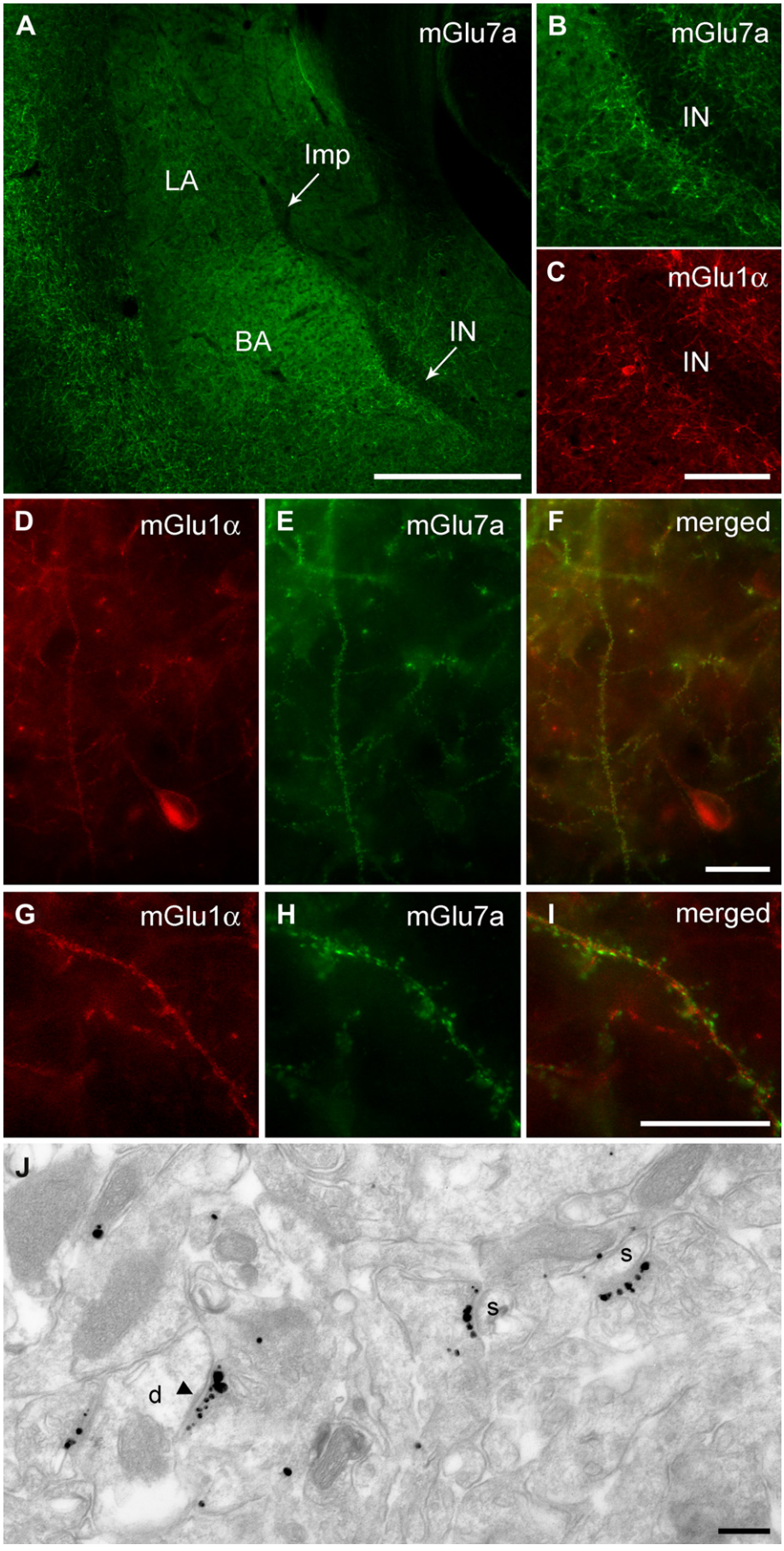
A
mGlu7a
LA
Imp
BA
IN
B
mGlu7a
IN
C
mGlu1α
IN
D
mGlu1α
E
mGlu7a
F
merged
G
mGlu1α
H
mGlu7a
I
merged
J
s
s
d

main nucleus. A large bundle of labelled axons entered the stria terminalis to leave the amygdala.

For this pathway, PHA-L and mGlu receptor immuno-electron microscopy was limited to the ITC (Fig. 9D–E). Although PHA-L labelled BA terminals in the ITC formed approximately 86% of synapses with dendritic spines, we observed a higher degree of synapses on dendritic shafts (14%), when compared to the other pathways analyzed. Of the shaft synapses 50% were symmetric, suggesting that some labelled interneurons of the BA anterogradely projected to the ITC. As shown in Table 2, ~20% of BA labelled terminals in the ITC possessed mGlu7a receptors presynaptically, of these 50% were in boutons targeting the shafts and 24% the spines of mGlu1α immunolabelled neurons. Conversely, BA inputs did not contain mGlu8a receptors.

4. Discussion

A full understanding of how a pharmacological treatment influences a specific behavioural response requires, among other aspects, the identification of the brain areas and neural circuitries expressing the drug target. Here, we showed that the activation of mGlu7 or mGlu8 receptors through specific agonists, administered intra-amygdala before extinction training, produced different effects on the conditioned response. The mGlu7 receptor agonist AMN082 facilitated extinction acquisition, whereas activation of mGlu8 receptors by (S)-3,4-DCPG prevented the reduction of the freezing behaviour normally observed by the re-exposure of the animals to the conditioning context in the absence of the unconditioned stimulus. Despite the relatively similar distribution of the immunoreactivity for mGlu7a and mGlu8a receptors within the BLA and ITCs (Masugi et al., 1999), our anatomical analysis at the ultrastructural level now revealed how these two receptors are to a significant extent segregated to different inputs. As shown schematically in Fig. 10, which tries to summarise our anatomical findings, mGlu7a receptors were located primarily onto glutamatergic afferents either intrinsic to the BLA or extrinsic and arising from the thalamus, but not the mPFC. On the other hand, mGlu8a showed a more restricted distribution than mGlu7a receptors in the BA and appeared absent from the three pathways that have been examined in this study. The identified segregation of these two group III mGlu receptors into primarily distinct afferents corroborates the marked pharmacological difference caused by their respective agonists on extinction training.

In the present study, the direct injection of AMN082 and (S)-3,4-DCPG into the BLA pre-empted the complicated interpretation of systemic administrations and removed the risk of confounding actions of these compounds on peripheral group III mGlu receptors (Julio-Pieper et al., 2011). Based on previous studies, we can assume that the area in which these drugs have exerted their effect remains probably restricted to less that 1 mm around the injection site (Palazzo et al., 2008, 2011). Therefore, the effect of AMN082 and (S)-3,4-DCPG should be confined primarily if not exclusively to the BLA and the surrounding ITCs. Moreover, we selected drug doses within the range of those previously used in other studies and shown to induce marked behavioural or physiological effects (Marabese et al., 2007; Palazzo et al., 2008). On the other hand, given the relatively high concentration of AMN082 and (S)-3,4-DCPG in the vicinity of the injection site a possible off site effect, e.g. on other mGlu receptors, cannot be ruled out. However, as the drugs were infused into the BLA at a very low speed and 15 min prior to the extinction training, we believe that significant off site effects influencing extinction training are unlikely.

Recently, group III mGlu receptors have received increasing attention as potential novel targets for anxiety disorders (Swanson et al., 2005). The overall effect mediated by these receptors appears to result from a complex balance between facilitatory and inhibitory actions that is dependent on their regulation of neurotransmitter release directly at the active zone of axon terminals. Indeed, we found that mGlu7a and mGlu8a receptors in the BLA and ITCs are exclusively located presynaptically in both glutamatergic and GABAergic terminals, similar to what observed in other brain areas (Ferraguti and Shigemoto, 2006; Ferraguti et al., 2005).

Only in the last few years, the individual role of distinct group III mGlu receptors has begun to emerge with the development of subtype selective drugs (Nicoletti et al., 2011). This study shows distinct roles of mGlu7 and mGlu8 in the expression of extinction and concurs with previous reports in delineating different functions for these receptors on a number of behavioural manifestations including pain modulation and anxiety (Marabese et al., 2007; Palazzo et al., 2008; Ren et al., 2011).

4.1. Potential neural mechanisms underlying enhanced extinction following intra-amygdala activation of mGlu7 receptors

Our behavioural findings, which demonstrate a facilitated acquisition of extinction of contextual fear by AMN082, are in agreement with the observed delayed extinction learning in mGlu7-deficient mice in both aversive and appetitive experimental paradigms (Callaerts-Vegh et al., 2006; Goddyn et al., 2008), as well as with the facilitated extinction of cue-induced fear-potentiated startle (Fendt et al., 2008). However, systemic administration of AMN082 in rats has been recently shown to attenuate within-session extinction, but to facilitate between-session extinction retention (Toth et al., 2012). The limited facilitatory effect of AMN082 on extinction acquisition observed in our study is likely due to the use of already well extinguishing mice. Since these animals show a very efficient extinction recall, it is difficult to demonstrate a further reduction of the freezing. This view is supported by additional evidence obtained with oral administration of AMN082 to 129/SvImJ mice, an animal model of impaired extinction (Hefner et al., 2008). In 129/SvImJ mice, AMN082 produced a significant improvement of both acquisition and consolidation of fear extinction (Whittle, Ferraguti and Singewald, personal communication). Taken together our results substantiate the view that memories can be more easily inhibited when mGlu7 receptors are activated (Fendt et al., 2008). One of the main conclusions of our study is that the facilitation of extinction occurs through the activation of mGlu7 receptors located within amygdala networks. Previous anatomical evidence has demonstrated that in the BLA mGlu7 had the highest density of all group III mGlu receptor subtypes (Corti et al., 1998; Kinoshita et al., 1998; Masugi et al., 1999; Shigemoto et al., 1997). Here, we reveal the precise localization of mGlu7 receptors in afferents to the BA and ITCs. These were primarily glutamatergic inputs originating from BA pyramidal neurons and the midline

Fig. 3. Distribution of mGlu7a receptors in the amygdala and preferential targeting of large mGlu1α+ ITC neurons. (A) Immunofluorescence micrograph showing intense punctate mGlu7a receptor reactivity in the BLA and in particular around the Imp and IN clusters. Scale bar: 500 μm. (B) This micrograph shows an enlarged view of the IN and the intense labelling around this cluster, but not inside, can be better appreciated. (C) Immunofluorescence micrograph taken at the same focal plane as (B) and showing mGlu1α receptor reactivity in the IN. Scale bar: 125 μm. (D–F) Low and (G–I) high magnification images depicting mGlu1α+ dendrites and spines of large ITC neurons decorated by dense mGlu7a positive terminals. Scale bar: D–I 20 μm. (J) Pre-embedding immunogold/silver labelling for mGlu7a receptors in the BA. Immunometal particles identifying mGlu7a receptors are selectively concentrated in the presynaptic active zone of axon terminals, which establish primarily excitatory synapses with postsynaptic dendrites (solid arrowhead) and spines. Scale bar: 500 nm. Abbreviations: BA, basal amygdala; d, dendrite; Imp, medial paracapsular ITC cluster; IN, main ITC nucleus; LA, lateral amygdala; s, spine.

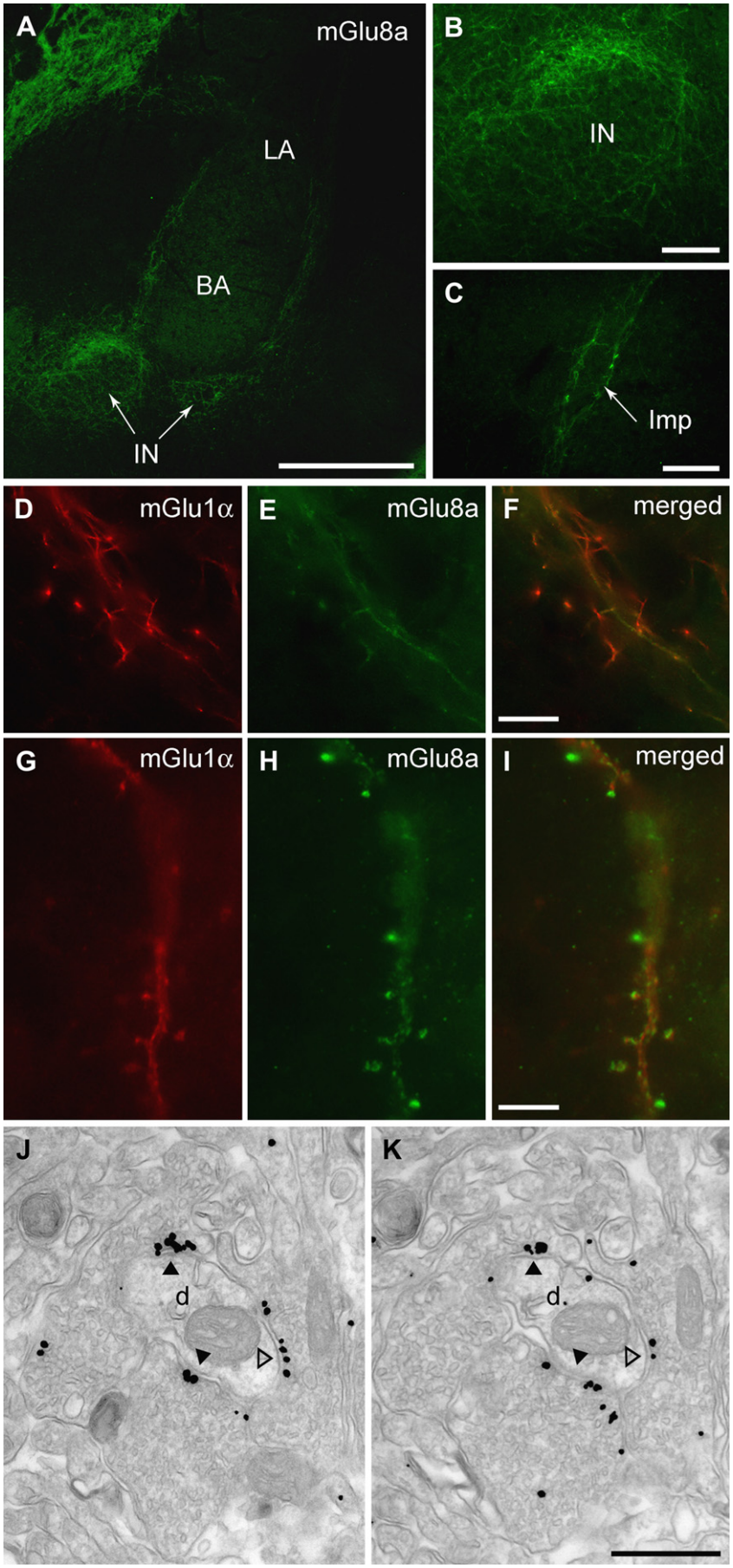
A
mGlu8a
LA
BA
IN
B
IN
C
Imp
D
mGlu1α
E
mGlu8a
F
merged
G
mGlu1α
H
mGlu8a
I
merged
J
d
K
d

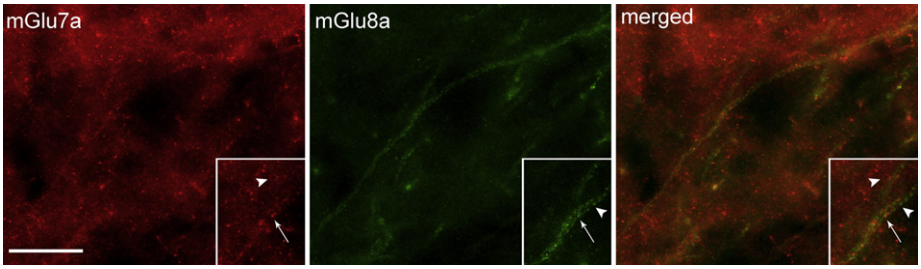

Fig. 5. Colocalization between mGlu7a and mGlu8a receptors on the large dendrite of a neuron located adjacent to the main ITC nucleus. The immunoreactivity for mGlu7a (shown in red) appears widespread whereas the immunoreactivity for mGlu8a (shown in green) is much more restricted and primarily decorates large dendrites. The insert shows a portion of a dendrite at higher magnification. The arrow indicates a bouton labelled for both receptors, whereas the arrowheads point to boutons labelled only for mGlu7a or mGlu8a. Scale bar: 20 μm.

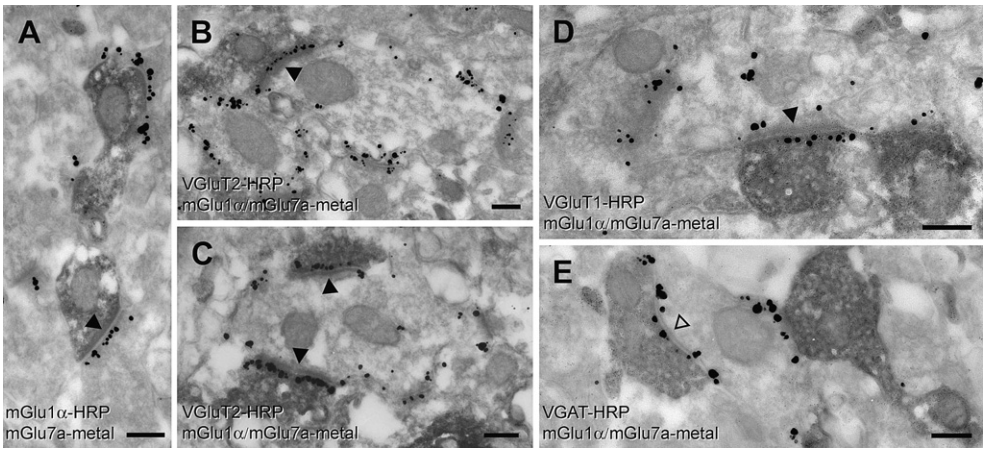

Fig. 6. Glutamatergic and GABAergic axon terminals innervating large mGlu1α+ ITC neurons contain mGlu7a receptors at their active zone. (A) Electron micrograph of a double pre-embedding immunoreaction in which a mGlu1α+ dendrite is revealed by horseradish peroxidase (HRP, diffuse electron dense reaction) whereas mGlu7a receptors are visualized by silver-intensified nanogold. Immunometal particles are clearly visible in the active zone of presynaptic terminals. (B–C) Electron micrographs of a triple pre-embedding immunoreaction in which the immunoreactivity for VGluT2 is shown by HRP, whereas immunometal particles on the postsynaptic membrane reveal mGlu1α receptors, and immunometal particles on the presynaptic membrane visualize mGlu7a receptors. Clear presynaptic labelling for mGlu7a receptors can be observed in the VGluT2+ (HRP) boutons forming asymmetric synapses (indicated by a solid arrowhead) with mGlu1α+ dendrites. (D) This electron micrograph shows the presence of mGlu7a receptors (immunometal particles) at the active zone of a VGluT1+ (HRP) axon terminal forming an asymmetric synapse (indicated by a solid arrowhead) with a mGlu1α+ dendrite. (E) In this electron micrograph the presence of mGlu7a receptors (immunometal particles) can be observed at the active zone of a VGAT+ (HRP) axon terminal forming a symmetric synapse (indicated by an empty arrowhead) with a mGlu1α+ dendrite. Scale bars: 200 nm.

thalamus, which contacted mostly spines. However, the relatively high number of asymmetric synapses on dendrites made by mGlu7 receptor-containing axon terminals suggests that they may originate from other brain areas with a preferential targeting onto dendrites. The BA and ITCs receive a prominent mesolimbic dopaminergic innervation (Fuxe et al., 2003). However, *in vivo* microdialysis studies showed that systemic administration of AMN082 did not influence extracellular dopamine (DA) levels (Li et al., 2008). Moreover, the ventral tegmental area and substantia nigra pars compacta possess negligible levels of mGlu7 receptor mRNA (Ohishi et al., 1995). Taken together these findings suggest that mGlu7 receptors are not present on DAergic terminals and that the facilitation of extinction by AMN082 is a DA-independent mechanism. Evidence from previous studies indicates that the modulation of the noradrenergic system within the BLA facilitates the expression and consolidation of extinction of contextual fear conditioning (Berlau and McGaugh, 2006; Morris and Bouton, 2007). The noradrenergic innervation of the BLA arises mainly from the locus coeruleus in the brain stem (Fallon et al., 1978; Pickel et al., 1974; Roder and Ciriello, 1993), a brain structure expressing very high levels of mGlu7 receptor transcripts (Ohishi et al., 1995). Moreover, noradrenergic axons in the BLA form both asymmetric and symmetric synapses primarily with dendrites (Li et al., 2001). Therefore, mGlu7 receptors, besides glutamatergic and GABAergic terminals, may be located also presynaptically on noradrenergic afferents to the BA and ITCs. Further studies addressing the distribution and role of mGlu7 receptors on the noradrenergic system in the amygdala are warranted. The localization of mGlu7 receptors in a number of different

Fig. 4. Distribution of mGlu8a receptors in the amygdala and preferential targeting of large mGlu1α+ ITC neurons. (A) Immunofluorescence micrograph showing intense mGlu8a receptor reactivity around the BLA and in particular enfolding ITC clusters. Scale bar: 500 μm. (B) This micrograph shows an enlarged view of the IN and the particularly intense labelling at the outer border of this cluster. Scale bar: 100 μm. (C) Likewise, intense mGlu8a receptor labelling can be appreciated around the Imp cluster. Scale bar: 100 μm. (D–F) Low and (G–I) high magnification images depicting mGlu1α+ dendrites and spines of large ITC neurons decorated by dense mGlu8a positive terminals. Scale bar: D–F, 20 μm; G–I, 15 μm. (J, K) Consecutive electron micrographs of a dendritic profile receiving both excitatory (solid arrowhead) and inhibitory (open arrowhead) synapses by axon terminals enriched in mGlu8a receptors (labelled by immunoglod particles) at their active zone. Scale bar: 500 nm. Abbreviations: BA, basal amygdala; d, dendrite; Imp, medial paracapsular ITC cluster; IN, main ITC nucleus; LA, lateral amygdala; s, spine.

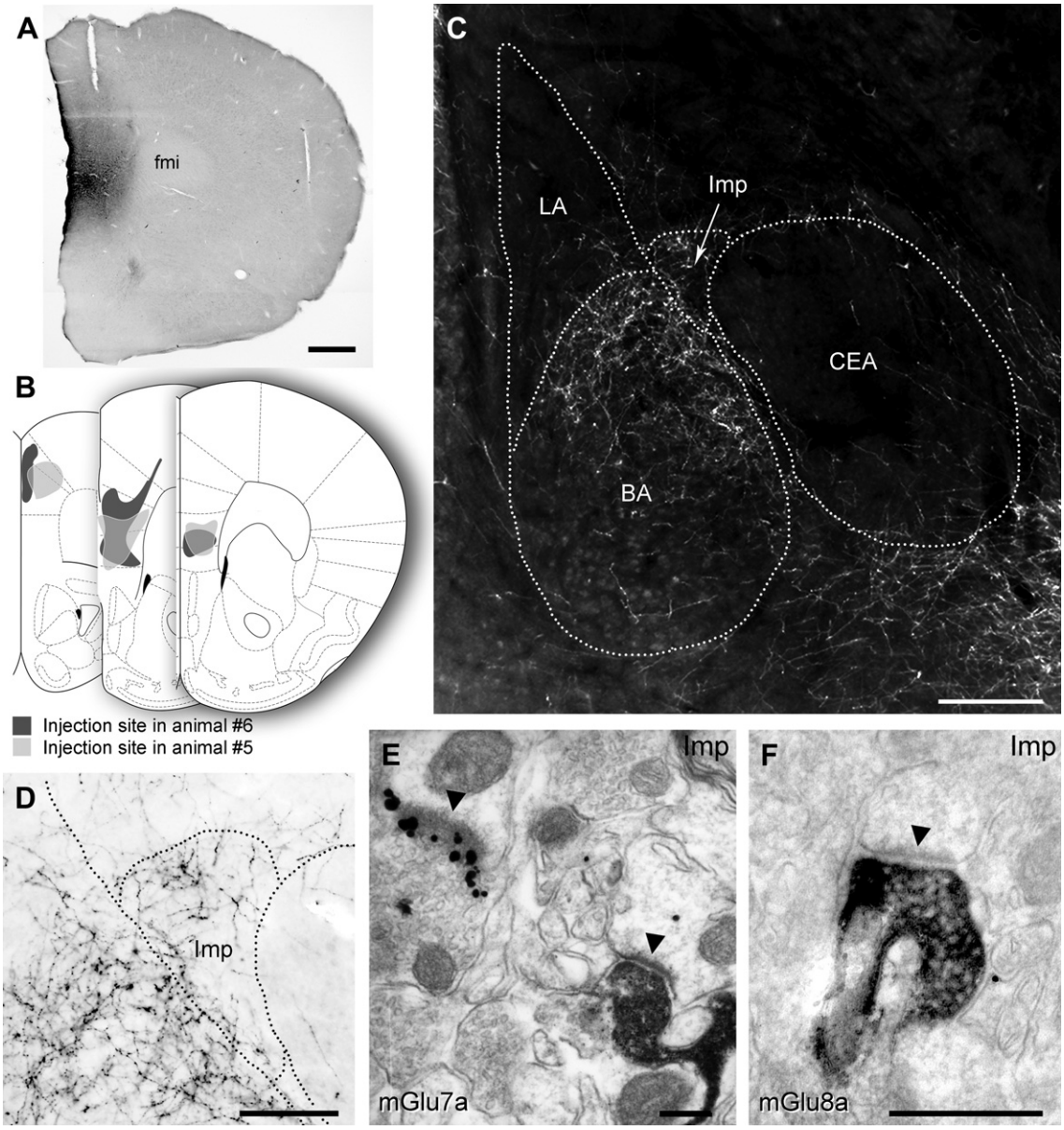

Fig. 7. Projections of the medial prefrontal cortex to the amygdala lack presynaptic mGlu7a and mGlu8a receptors. (A) Photomicrograph showing a PHA-L injection site in the mPFC (mouse #5). (B) Line drawings of coronal sections arranged caudorostrally showing the extent of the PHA-L injection in the mPFC for the two selected cases. Each injection is illustrated with a different shading pattern. Although both injections are preferentially located within the infralimbic mPFC a few labelled neurons could also be observed in the prelimbic area. (C) Darkfield photomicrograph showing the distribution of labelled fibres in the amygdala. (D) Higher power photomicrograph showing mPFC labelled axons in the Imp and intermediate division of the BA. (E) Electron micrograph of a PHA-L-labelled mPFC terminal (filled by a dark electron dense reaction product) immunonegative for mGlu7a receptor and forming an asymmetric synapse (indicated by an arrowhead) with a small dendrite of an ITC neuron in the Imp. Nearby a large terminal shows an intense mGlu7a receptor labelling (immunometal particles) at its active zone. This terminal forms an asymmetric synapse (indicated by an arrowhead) with a small dendrite and lacks PHA-L labelling. (F) Electron micrograph of a PHA-L-labelled mPFC terminal (filled by a dark electron dense reaction product) immunonegative for mGlu8a receptor and forming an asymmetric synapse (indicated by an arrowhead) with a dendritic spine of an ITC neuron in the Imp. Abbreviations: BA, basal nucleus of the amygdala; CEA, central nucleus of the amygdala; fmi, forceps minor corpus callosum; Imp, medial paracapsular cluster; LA, lateral nucleus of the amygdala; Scale bars: A, 500 μm; C, 200 μm; D, 100 μm; E, 200 nm; F, 500 nm.

afferents to both BA and ITC neurons makes it difficult to relate the behavioural effects elicited by AMN082 to a definite network. On the other hand, our study confines the presence of mGlu7 receptors to a few defined inputs and rules out an action of AMN082 on mPFC inputs, and in particular those of the IL-PFC known to be important for the long-term storage of fear extinction memories (Quirk and Mueller, 2008).

The facilitation of extinction acquisition mediated by AMN082, besides being possibly due to an activity-dependent depression of neurotransmission (Perroy et al., 2002; Ugolini et al., 2008), could also be ascribed to a functional blockade of mGlu7 receptors. In fact, it has been shown that AMN082 in addition to stimulating can induce the internalization of mGlu7 receptors (Pelkey et al., 2007). However, since the selective downregulation of mGlu7 receptor mRNA expression by means of short interfering RNAs inhibited the extinction of fear-potentiated startle, whereas AMN082 given systemically facilitated extinction of conditioned fear (Fendt et al., 2008), a functional blockade of the receptor appears unlikely.

Table 2
Quantitative evaluation of PHA-L-labelled inputs containing mGlu7a or mGlu8a receptors and their respective targets in the ITCs and BA.

		PHA-L-positive boutons							
		mGlu7a+		mGlu8a+		On mGlu1a+ profiles		mGlu7a+ on mGlu1a+ profiles	
		%	(*n*)	%	(*n*)	%	(*n*)	%	(*n*)
Inputs to ITCs									
mPFC projections	Dendrites	0%	0/1	0%	0/2	0%	0/3	–	
	Spines	0%	0/61	0%	0/35	9%	9/96	0%	0/6
Thalamic projections	Dendrites	0%	0/2	0%	0/1	0%	0/3	0%	0/1
	Spines	23%	10/44	0%	0/16	38%	23/60	29%	5/17
BA projections	Dendrites	20%	1/5[a]	0%	0/12[a]	29%	5/17	50%	1/2
	Spines	20%	12/61	0%	0/45	37%	39/106	24%	9/38
Inputs to BA									
mPFC projections	Dendrites	0%	0/2	–	–	0%	0/1	0%	0/1
	Spines	0%	0/37	0%	0/31	18%	12/68	0%	0/9
Thalamic projections	Dendrites	29%	2/7	0%	0/5	25%	3/12	33%	1/3
	Spines	7%	5/71	0%	0/48	24%	29/119	8%	2/25
	Soma	0%	0/1	–		–		–	

(*n*) Number of positive profiles over the overall number of synapses observed.
Data have been collected from 2 animals for each pathway and at least 2 blocks per animal.
[a] For PHA-L-labelled BA projections also symmetric synapses on dendrites have been observed. In particular, $n = 1$ in the reaction for mGlu7a and $n = 2$ in that for mGlu8a.

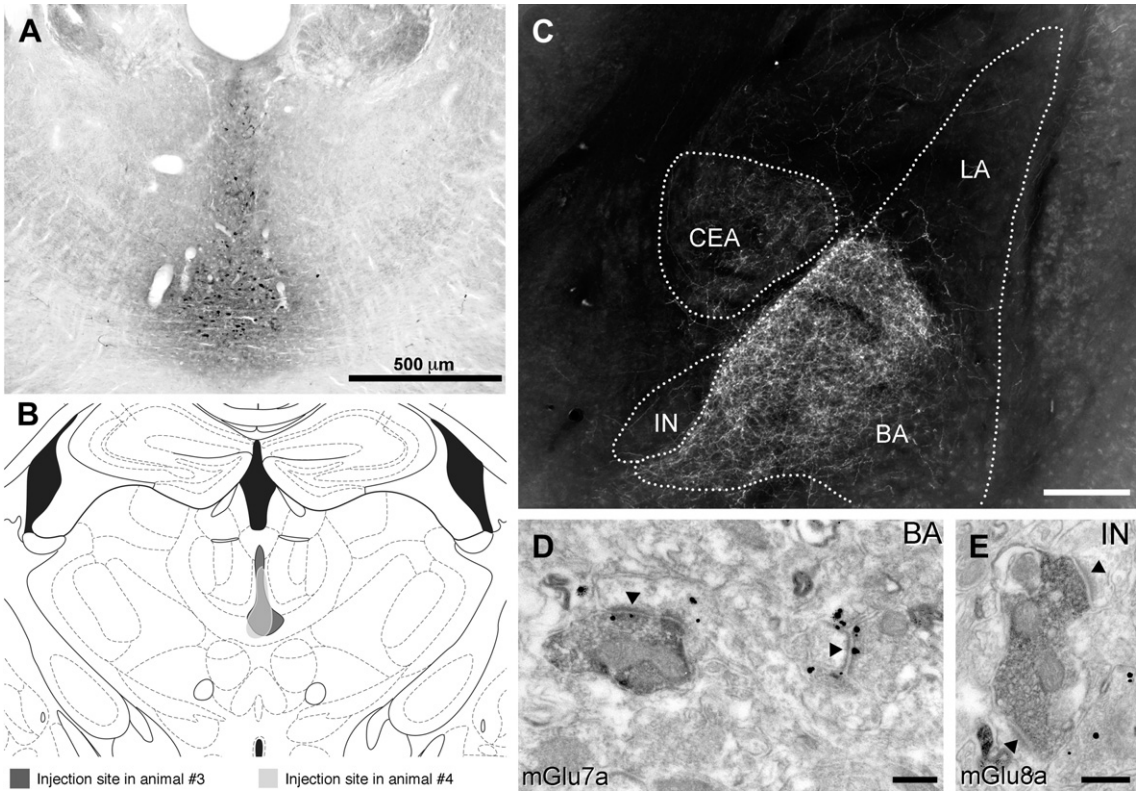

Fig. 8. Thalamic midline efferents to the amygdala contain presynaptic mGlu7a, but not mGlu8a receptors. (A) Photomicrograph showing a PHA-L injection site in the thalamic midline nuclei (mouse #3). (B) Line drawings of a coronal section showing the extent of the PHA-L injection in the thalamus for the two selected cases. Each injection is illustrated with a different shading pattern. Both injections largely overlap and are primarily located within the paraventricular, intermediodorsal and central medial thalamic nuclei. (C) Darkfield photomicrograph showing the distribution of PHA-L-labelled fibres in the amygdala. The terminal zone appears predominantly intense in the intermediate subdivision of the BA, moderate in the lateral division of the central nucleus and a few labelled axons can be observed in the main ITC nucleus and in the intermediate capsule. (D) Electron micrograph of a PHA-L-labelled thalamic terminal (filled by a dark electron dense reaction product) immunopositive for mGlu7a receptor (immunometal particles are visible at the active zone) and forming an asymmetric synapse (indicated by an arrowhead) with a large spine of a BA neuron. Nearby another axon terminal also showing presynaptic mGlu7a receptor labelling (immunometal particles) forms an asymmetric synapse (indicated by an arrowhead) with a small spine and lacks PHA-L labelling. This spine shows immunometal particles at its plasma membrane indicative of mGlu1α receptor labelling. (F) Electron micrograph of a PHA-L-labelled thalamic axon terminal (filled by a dark electron dense reaction product) immunonegative for mGlu8a receptor and forming two asymmetric synapses (indicated by arrowheads) with dendritic spines of an ITC neuron in the IN. Abbreviations: BA, basal nucleus of the amygdala; CEA, central nucleus of the amygdala; Imp, medial paracapsular ITC cluster; IN, main ITC nucleus; LA, lateral nucleus of the amygdala. Scale bars: A, 500 μm; C, 200 μm; D, 200 nm; E, 250 nm.

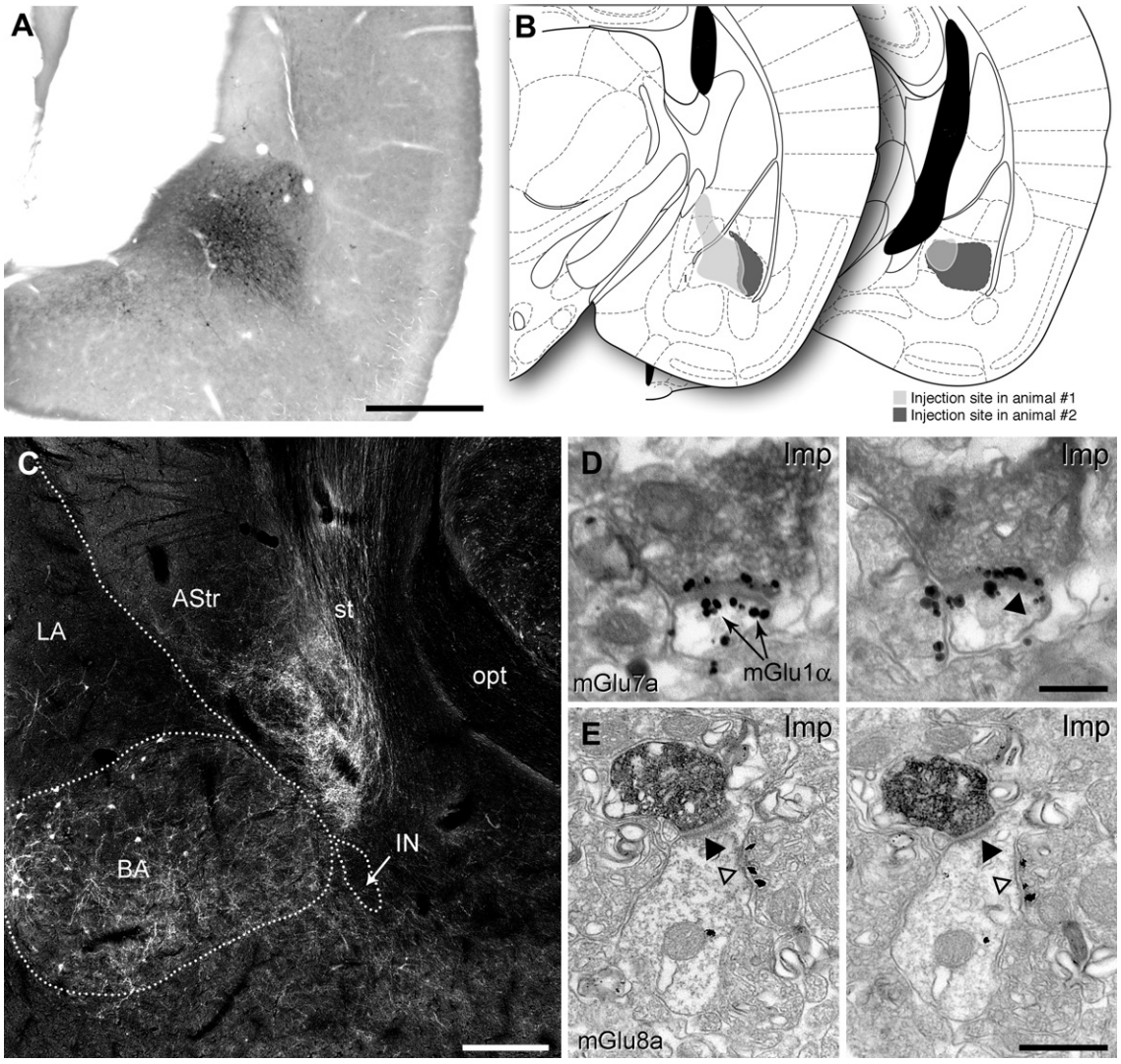

Fig. 9. Intrinsic projections of the basolateral amygdala possess mGlu7a but not mGlu8a receptors. (A) Photomicrograph showing a PHA-L injection site in the caudal portion of the BA (mouse #2). (B) Line drawings of coronal sections arranged rostrocaudally showing the extent of the PHA-L injection in the BA for the two selected cases. Each injection is illustrated with a different shading pattern. (C) Darkfield photomicrograph showing the distribution of PHA-L-labelled fibres in the amygdala. The terminal zone appears predominantly intense in the BA, where a number of retrogradely labelled neurons can also be observed. A large number of PHA-L-labelled fibres enter the stria terminalis. (D) Serial electron micrographs of a PHA-L-labelled BA axon terminal (filled by a dark electron dense reaction product) intensely immunopositive for mGlu7a receptor (immunometal particles are visible at the active zone) and forming an asymmetric synapse (indicated by an arrowhead) with a small dendrite of an Imp ITC neuron also immunoreactive for the mGlu1α receptor (immunometal particles are visible at the plasma membrane outside the postsynaptic density; arrows). (E) Serial electron micrographs of a PHA-L-labelled BA axon terminal (filled by a dark electron dense reaction product) immunonegative for mGlu8a receptor and forming an asymmetric synapse (indicated by a solid arrowhead) with a dendrite of an ITC neuron in the Imp. The same dendrite also receives a mGlu8a receptor-labelled bouton forming a symmetric synapse (indicated by an empty arrowhead). Abbreviations: AStr, amygdala–striatum transition zone; BA, basal nucleus of the amygdala; IN, main ITC nucleus; LA, lateral nucleus of the amygdala; opt, optic tract; st, stria terminalis. Scale bars: A, 500 μm; C, 200 μm; D, 200 nm; E, 500 nm.

4.2. Potential neural mechanisms underlying impaired extinction following intra-amygdala activation of mGlu8 receptors

The present study demonstrates that (S)-3,4-DCPG, when injected intra-amygdala, precluded the attenuation of the freezing response during the extinction training in mice, but did not prevent the formation and consolidation of an extinction memory since the level of freezing in extinction recall was comparable to the control group. (S)-3,4-DCPG also caused a reduced spontaneous locomotor activity and a short lasting immobility that was not due to motor impairment or sedation, as indicated by the rotarod test. These behavioural effects suggest an anxiogenic-like activity of (S)-3,4-DCPG that influenced fear behaviour and concealed the behavioural expression of fear extinction rather than impairing it. Interestingly, this seems in line with the impaired fear extinction shown by animals characterized by enhanced trait anxiety (Muigg et al., 2008), which also closely mirrors findings in anxiety patients (Lissek et al., 2005). At odds with our findings, (S)-3,4-DCPG was found to exert anxiolytic-like activity when given systemically in mice (Duvoisin et al., 2010). However, systemic application of (S)-3,4-DCPG might have influenced a number of areas other than the BLA (Gosnell et al., 2011), and thus yielded a different net effect compared to a local injection. No help for interpretation of our data can be gained from studies on anxiety-like behaviour in mGlu8-deficient mice as they gave rise to largely conflicting results. In fact, some of these studies reported an anxiogenic-like phenotype in mGlu8-null mice (Duvoisin et al., 2005; Linden et al., 2002; Robbins et al., 2007), whereas others

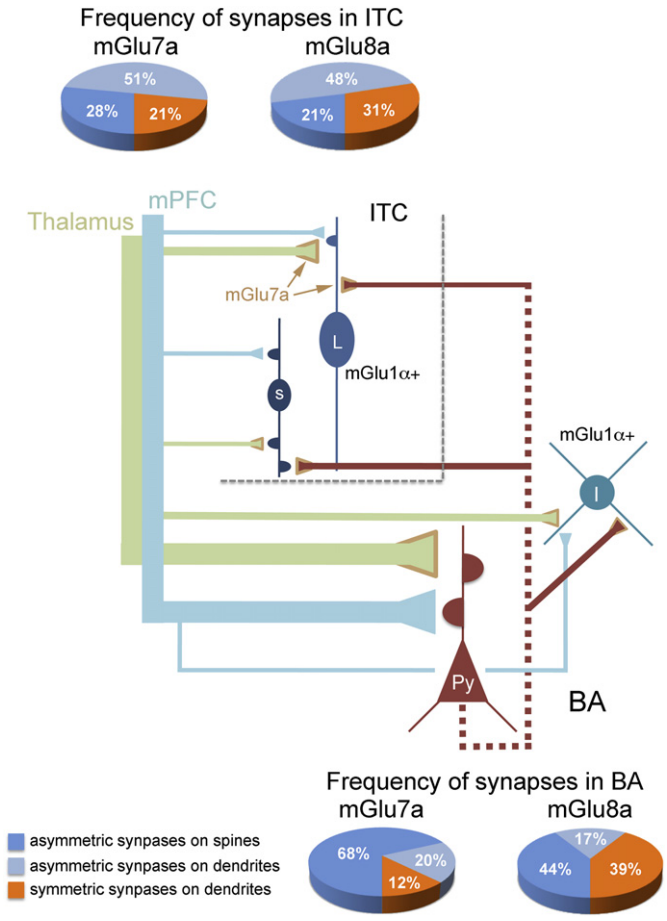

Fig. 10. Schematic representation of the pathways arising from the dorsal subdivision of the thalamic midline nuclei (green), medial prefrontal cortex (mPFC, light blue) or caudal portion of the basal nucleus of the amygdala (BA, red) by means of anterograde tracing, and targeting: pyramidal neurons (Py) and interneurons expressing mGlu1α receptors (I) in the BA; or medium-spiny (s) and large (L) mGlu1α+ neurons in the ITCs. The size of the inputs is roughly proportional to their relative density. The selective presence of presynaptic mGlu7a receptors at specific pathways is shown by a light brown contour (as indicated by arrows). The respective frequency of asymmetric synapses on spines or dendrites as well as symmetric synapses formed by presynaptic axon terminals containing mGlu7a or mGlu8a receptors in the ITCs (upper pie diagrams) and BA (lower pie diagrams) is also shown.

found no effect of the genotype on measures of anxiety (Fendt et al., 2010; Gerlai et al., 2002). Injection of (S)-3,4-DCPG in the rat BLA showed no effect in the elevated plus maze and Vogel test (Palazzo et al., 2008; Stachowicz et al., 2005), but spontaneous locomotor activity and extinction of fear conditioning were not analyzed. Although these data might question an effect of (S)-3,4-DCPG on measures of anxiety upon local infusion in the BLA, we cannot exclude that differences in doses, tests used and species contributed to these apparently incongruous findings.

Our study reveals a more restricted distribution of mGlu8a in the BLA compared to mGlu7a receptors, but a similarly intense decoration of large mGlu1α+ neurons at the border of ITC clusters. None of the traced pathways appeared to contain detectable amounts of mGlu8a receptors, thus leaving still open the precise identification of the source of the inputs enriched in these receptors. Therefore, even though we cannot confine the behavioural effects of (S)-3,4-DCPG to a definite amygdala network, our work suggests that the mGlu8a-containing inputs forming asymmetric synapses mostly arise from areas extrinsic to the amygdala, which could include the somatosensory, perirhinal and/or piriform cortex or the ventromedial nucleus of the hypothalamus. In fact, among the few areas expressing significant amounts of mGlu8a mRNA (Corti et al., 1998; Saugstad et al., 1997), these appear the only ones to provide a significant source of axons to the BLA (Pitkänen, 2000). On the other hand, the large percentage of symmetric synapses on dendrites of BLA neurons made by mGlu8a-containing inputs may derive from local interneurons, consistent with the moderate expression of mGlu8a mRNA in the BLA (Corti et al., 1998). Further tracing studies combined with immuno-electron microscopy are needed to finally reveal the exact source of mGlu8+ inputs.

4.3. Selective targeting of mGlu1α+ large ITC neurons by axon terminals enriched in mGlu7a and/or mGlu8s receptors

One of the main findings of this work is the selective targeting by axon terminals enriched in group III mGlu receptors of the large mGlu1α+ neurons found at the border of ITC clusters (Busti et al., 2011). The extensive dendritic arbors of these neurons mostly align along the intermediate capsule and are probably capable of receiving and integrating a large variety of inputs. Most of these inputs appear to contain mGlu7a and/or mGlu8a receptors. Indeed, we have shown that the mGlu7a receptor is present in both GABAergic and glutamatergic afferents, and that the latter ones form synapses primarily with the dendritic shafts, in agreement with the poorly-spiny nature of these ITC neurons.

Interestingly, both short- and long-term extinction, but not fear acquisition, was found impaired after injection of a mGlu1 receptor antagonist into the BLA (Kim et al., 2007). Moreover, systemic pharmacologic blockade of mGlu1 receptors before extinction retrieval facilitated relapse phenomena, such as renewal and reinstatement (Clem and Huganir, 2010). Taken together these data suggest that the activity of mGlu1 receptors is linked specifically to mechanisms underlying fear extinction. Although the exact cellular and molecular mechanisms underlying the role of mGlu1 receptors on extinction of fear conditioning remain to be established, our finding that large mGlu1α+ ITC neurons are recipient of heavy innervation by inputs from the thalamus, BA and mPFC as well as by afferents enriched in group III mGlu receptors, which themselves influence fear extinction, identifies them as a potential key component of the neural networks underlying fear extinction. Future studies are warranted to assess the projections and targets of these neurons.

5. Conclusions

The current pharmacotherapy of anxiety disorders primarily targets the GABAergic and serotonergic systems. However, these treatments appear of limited efficacy (Pull, 2007) underlying the need for treatments that address novel mechanisms. In addition, pharmacological treatments that could be used in adjunct to behavioural therapy to facilitate extinction would be of particularly clinical interest. Our study substantiates the view that mGlu7 receptor agonists or positive allosteric modulators may represent such a class of drugs. Moreover, the elucidation of how and where, at the synaptic level, group III mGlu receptors may impinge on the neural pathways within the amygdala underlying inhibition of fear, will help determining the therapeutic value of drugs acting at these receptors.

Acknowledgements

We would like to thank Michaela Benedet and Johannes Pallua for helping with the electron microscopic analysis of tract tracing

experiments; Gabi Schmidt for excellent technical support; M. Watanabe (Dept. Anatomy, Hokkaido University, Sapporo, Japan) for kindly providing VGluT1, VGluT2, VGAT and mGlu1α receptor antibodies. This work was supported by the grants from the Austrian Science Fund (FWF): I252-B18 and W01206-10 to F.F., and SFB F4410 to N.S.

References

Amano, T., Unal, C.T., Pare, D., 2010. Synaptic correlates of fear extinction in the amygdala. Nat. Neurosci. 13, 489–494.
Berlau, D.J., McGaugh, J.L., 2006. Enhancement of extinction memory consolidation: the role of the noradrenergic and GABAergic systems within the basolateral amygdala. Neurobiol. Learn. Mem. 86, 123–132.
Busti, D., Geracitano, R., Whittle, N., Dalezios, Y., Manko, M., Kaufmann, W., Satzler, K., Singewald, N., Capogna, M., Ferraguti, F., 2011. Different fear states engage distinct networks within the intercalated cell clusters of the amygdala. J. Neurosci. 31, 5131–5144.
Callaerts-Vegh, Z., Beckers, T., Ball, S.M., Baeyens, F., Callaerts, P.F., Cryan, J.F., Molnar, E., D'Hooge, R., 2006. Concomitant deficits in working memory and fear extinction are functionally dissociated from reduced anxiety in metabotropic glutamate receptor 7-deficient mice. J. Neurosci. 26, 6573–6582.
Clem, R.L., Huganir, R.L., 2010. Calcium-permeable AMPA receptor dynamics mediate fear memory erasure. Science 330, 1108–1112.
Corti, C., Restituito, S., Rimland, J.M., Brabet, I., Corsi, M., Pin, J.P., Ferraguti, F., 1998. Cloning and characterization of alternative mRNA forms for the rat metabotropic glutamate receptors mGluR7 and mGluR8. Eur. J. Neurosci. 10, 3629–3641.
Duvoisin, R.M., Zhang, C., Pfankuch, T.F., O'Connor, H., Gayet-Primo, J., Quraishi, S., Raber, J., 2005. Increased measures of anxiety and weight gain in mice lacking the group III metabotropic glutamate receptor mGluR8. Eur. J. Neurosci. 22, 425–436.
Duvoisin, R.M., Pfankuch, T., Wilson, J.M., Grabell, J., Chhajlani, V., Brown, D.G., Johnson, E., Raber, J., 2010. Acute pharmacological modulation of mGluR8 reduces measures of anxiety. Behav. Brain Res. 212, 168–173.
Ehrlich, I., Humeau, Y., Grenier, F., Ciocchi, S., Herry, C., Luthi, A., 2009. Amygdala inhibitory circuits and the control of fear memory. Neuron 62, 757–771.
Fallon, J.H., Koziell, D.A., Moore, R.Y., 1978. Catecholamine innervation of the basal forebrain. II. Amygdala, suprarhinal cortex and entorhinal cortex. J. Comp. Neurol. 180, 509–532.
Fanselow, M.S., 1980. Conditioned and unconditional components of post-shock freezing. Pavlov J. Biol. Sci. 15, 177–182.
Fendt, M., et al., 2008. mGluR7 facilitates extinction of aversive memories and controls amygdala plasticity. Mol. Psychiatry 13, 970–979.
Fendt, M., Burki, H., Imobersteg, S., van der Putten, H., McAllister, K., Leslie, J.C., Shaw, D., Holscher, C., 2010. The effect of mGlu8 deficiency in animal models of psychiatric diseases. Genes Brain Behav. 9, 33–44.
Ferraguti, F., Shigemoto, R., 2006. Metabotropic glutamate receptors. Cell Tissue Res. 326, 483–504.
Ferraguti, F., Cobden, P., Pollard, M., Cope, D., Shigemoto, R., Watanabe, M., Somogyi, P., 2004. Immunolocalization of metabotropic glutamate receptor 1alpha (mGluR1alpha) in distinct classes of interneuron in the CA1 region of the rat hippocampus. Hippocampus 14, 193–215.
Ferraguti, F., Klausberger, T., Cobden, P., Baude, A., Roberts, J.D., Szucs, P., Kinoshita, A., Shigemoto, R., Somogyi, P., Dalezios, Y., 2005. Metabotropic glutamate receptor 8-expressing nerve terminals target subsets of GABAergic neurons in the hippocampus. J. Neurosci. 25, 10520–10536.
Fuxe, K., Jacobsen, K.X., Hoistad, M., Tinner, B., Jansson, A., Staines, W.A., Agnati, L.F., 2003. The dopamine D1 receptor-rich main and paracapsular intercalated nerve cell groups of the rat amygdala: relationship to the dopamine innervation. Neuroscience 119, 733–746.
Geracitano, R., Kaufmann, W.A., Szabo, G., Ferraguti, F., Capogna, M., 2007. Synaptic heterogeneity between mouse paracapsular intercalated neurons of the amygdala. J. Physiol. 585, 117–134.
Gerlai, R., Adams, B., Fitch, T., Chaney, S., Baez, M., 2002. Performance deficits of mGluR8 knockout mice in learning tasks: the effects of null mutation and the background genotype. Neuropharmacology 43, 235–249.
Goddyn, H., Callaerts-Vegh, Z., Stroobants, S., Dirikx, T., Vansteenwegen, D., Hermans, D., van der Putten, H., D'Hooge, R., 2008. Deficits in acquisition and extinction of conditioned responses in mGluR7 knockout mice. Neurobiol. Learn. Mem. 90, 103–111.
Goosens, K.A., Maren, S., 2001. Contextual and auditory fear conditioning are mediated by the lateral, basal, and central amygdaloid nuclei in rats. Learn. Mem. 8, 148–155.
Gosnell, H.B., Silberman, Y., Grueter, B.A., Duvoisin, R.M., Raber, J., Winder, D.G., 2011. mGluR8 modulates excitatory transmission in the bed nucleus of the stria terminalis in a stress-dependent manner. Neuropsychopharmacology 36, 1599–1607.
Gu, G.B., Simerly, R.B., 1997. Projections of the sexually dimorphic anteroventral periventricular nucleus in the female rat. J. Comp. Neurol. 384, 142–164.
Hefner, K., Whittle, N., Juhasz, J., Norcross, M., Karlsson, R.M., Saksida, L.M., Bussey, T.J., Singewald, N., Holmes, A., 2008. Impaired fear extinction learning and cortico-amygdala circuit abnormalities in a common genetic mouse strain. J. Neurosci. 28, 8074–8085.
Herry, C., Ferraguti, F., Singewald, N., Letzkus, J.J., Ehrlich, I., Luthi, A., 2010. Neuronal circuits of fear extinction. Eur. J. Neurosci. 31, 599–612.
Julio-Pieper, M., Flor, P.J., Dinan, T.G., Cryan, J.F., 2011. Exciting times beyond the brain: metabotropic glutamate receptors in peripheral and non-neural tissues. Pharmacol. Rev. 63, 35–58.
Kim, J., Lee, S., Park, H., Song, B., Hong, I., Geum, D., Shin, K., Choi, S., 2007. Blockade of amygdala metabotropic glutamate receptor subtype 1 impairs fear extinction. Biochem. Biophys. Res. Commun. 355, 188–193.
Kinoshita, A., Ohishi, H., Neki, A., Nomura, S., Shigemoto, R., Takada, M., Nakanishi, S., Mizuno, N., 1996. Presynaptic localization of a metabotropic glutamate receptor, mGluR8, in the rhinencephalic areas: a light and electron microscope study in the rat. Neurosci. Lett. 207, 61–64.
Kinoshita, A., Shigemoto, R., Ohishi, H., van der Putten, H., Mizuno, N., 1998. Immunohistochemical localization of metabotropic glutamate receptors, mGluR7a and mGluR7b, in the central nervous system of the adult rat and mouse: a light and electron microscopic study. J. Comp. Neurol. 393, 332–352.
Lenth, R., 2006-9. Java Applets for Power and Sample Size [Computer Software].
Li, R., Nishijo, H., Wang, Q., Uwano, T., Tamura, R., Ohtani, O., Ono, T., 2001. Light and electron microscopic study of cholinergic and noradrenergic elements in the basolateral nucleus of the rat amygdala: evidence for interactions between the two systems. J. Comp. Neurol. 439, 411–425.
Li, X., Gardner, E.L., Xi, Z.X., 2008. The metabotropic glutamate receptor 7 (mGluR7) allosteric agonist AMN082 modulates nucleus accumbens GABA and glutamate, but not dopamine, in rats. Neuropharmacology 54, 542–551.
Likhtik, E., Popa, D., Apergis-Schoute, J., Fidacaro, G.A., Pare, D., 2008. Amygdala intercalated neurons are required for expression of fear extinction. Nature 454, 642–645.
Linden, A.M., Johnson, B.G., Peters, S.C., Shannon, H.E., Tian, M., Wang, Y., Yu, J.L., Koster, A., Baez, M., Schoepp, D.D., 2002. Increased anxiety-related behavior in mice deficient for metabotropic glutamate 8 (mGlu8) receptor. Neuropharmacology 43, 251–259.
Lissek, S., Powers, A.S., McClure, E.B., Phelps, E.A., Woldehawariat, G., Grillon, C., Pine, D.S., 2005. Classical fear conditioning in the anxiety disorders: a meta-analysis. Behav. Res. Ther. 43, 1391–1424.
Mahan, A.L., Ressler, K.J., 2012. Fear conditioning, synaptic plasticity and the amygdala: implications for posttraumatic stress disorder. Trends Neurosci. 35, 24–35.
Manko, M., Geracitano, R., Capogna, M., 2011. Functional connectivity of the main intercalated nucleus of the mouse amygdala. J. Physiol. 589, 1911–1925.
Marabese, I., et al., 2007. Periaqueductal gray metabotropic glutamate receptor subtype 7 and 8 mediate opposite effects on amino acid release, rostral ventromedial medulla cell activities, and thermal nociception. J. Neurophysiol. 98, 43–53.
Masugi, M., Yokoi, M., Shigemoto, R., Muguruma, K., Watanabe, Y., Sansig, G., van der Putten, H., Nakanishi, S., 1999. Metabotropic glutamate receptor subtype 7 ablation causes deficit in fear response and conditioned taste aversion. J. Neurosci. 19, 955–963.
McDonald, A.J., Mascagni, F., Guo, L., 1996. Projections of the medial and lateral prefrontal cortices to the amygdala: a *Phaseolus vulgaris* leucoagglutinin study in the rat. Neuroscience 71, 55–75.
Morris, R.W., Bouton, M.E., 2007. The effect of yohimbine on the extinction of conditioned fear: a role for context. Behav. Neurosci. 121, 501–514.
Muigg, P., Hetzenauer, A., Hauer, G., Hauschild, M., Gaburro, S., Frank, E., Landgraf, R., Singewald, N., 2008. Impaired extinction of learned fear in rats selectively bred for high anxiety – evidence of altered neuronal processing in prefrontal-amygdala pathways. Eur. J. Neurosci. 28, 2299–2309.
Muller, J., Corodimas, K.P., Fridel, Z., LeDoux, J.E., 1997. Functional inactivation of the lateral and basal nuclei of the amygdala by muscimol infusion prevents fear conditioning to an explicit conditioned stimulus and to contextual stimuli. Behav. Neurosci. 111, 683–691.
Myers, K.M., Davis, M., 2007. Mechanisms of fear extinction. Mol. Psychiatry 12, 120–150.
Nicoletti, F., Bockaert, J., Collingridge, G.L., Conn, P.J., Ferraguti, F., Schoepp, D.D., Wroblewski, J.T., Pin, J.P., 2011. Metabotropic glutamate receptors: from the workbench to the bedside. Neuropharmacology 60, 1017–1041.
Ohishi, H., Akazawa, C., Shigemoto, R., Nakanishi, S., Mizuno, N., 1995. Distributions of the mRNAs for L-2-amino-4-phosphonobutyrate-sensitive metabotropic glutamate receptors, mGluR4 and mGluR7, in the rat brain. J. Comp. Neurol. 360, 555–570.
Ottersen, O.P., Ben-Ari, Y., 1979. Afferent connections to the amygdaloid complex of the rat and cat. I. Projections from the thalamus. J. Comp. Neurol. 187, 401–424.
Palazzo, E., Fu, Y., Ji, G., Maione, S., Neugebauer, V., 2008. Group III mGluR7 and mGluR8 in the amygdala differentially modulate nocifensive and affective pain behaviors. Neuropharmacology 55, 537–545.
Palazzo, E., Marabese, I., Soukupova, M., Luongo, L., Boccella, S., Giordano, C., de Novellis, V., Rossi, F., Maione, S., 2011. Metabotropic glutamate receptor subtype 8 in the amygdala modulates thermal threshold, neurotransmitter release, and rostral ventromedial medulla cell activity in inflammatory pain. J. Neurosci. 31, 4687–4697.
Pape, H.C., Pare, D., 2010. Plastic synaptic networks of the amygdala for the acquisition, expression, and extinction of conditioned fear. Physiol. Rev. 90, 419–463.
Paxinos, G., Franklin, K.B.J., 2001. The Mouse Brain in Stereotaxic Coordinates. Academic Press.

Pelkey, K.A., Yuan, X., Lavezzari, G., Roche, K.W., McBain, C.J., 2007. mGluR7 undergoes rapid internalization in response to activation by the allosteric agonist AMN082. Neuropharmacology 52, 108–117.
Perroy, J., Richard, S., Nargeot, J., Bockaert, J., Fagni, L., 2002. Permissive effect of voltage on mGlu 7 receptor subtype signaling in neurons. J. Biol. Chem. 277, 1223–1228.
Phelps, E.A., Delgado, M.R., Nearing, K.I., LeDoux, J.E., 2004. Extinction learning in humans: role of the amygdala and vmPFC. Neuron 43, 897–905.
Pickel, V.M., Segal, M., Bloom, F.E., 1974. A radioautographic study of the efferent pathways of the nucleus locus coeruleus. J. Comp. Neurol. 155, 15–42.
Pitkänen, A., 2000. Connectivity of the Rat Amygdaloid Complex. Oxford University Press, Oxford.
Pull, C.B., 2007. Combined pharmacotherapy and cognitive-behavioural therapy for anxiety disorders. Curr. Opin. Psychiatry 20, 30–35.
Quirk, G.J., Beer, J.S., 2006. Prefrontal involvement in the regulation of emotion: convergence of rat and human studies. Curr. Opin. Neurobiol. 16, 723–727.
Quirk, G.J., Mueller, D., 2008. Neural mechanisms of extinction learning and retrieval. Neuropsychopharmacology 33, 56–72.
Ren, W., Palazzo, E., Maione, S., Neugebauer, V., 2011. Differential effects of mGluR7 and mGluR8 activation on pain-related synaptic activity in the amygdala. Neuropharmacology 61, 1334–1344.
Robbins, M.J., et al., 2007. Evaluation of the mGlu8 receptor as a putative therapeutic target in schizophrenia. Brain Res. 1152, 215–227.
Roder, S., Ciriello, J., 1993. Innervation of the amygdaloid complex by catecholaminergic cell groups of the ventrolateral medulla. J. Comp. Neurol. 332, 105–122.
Royer, S., Martina, M., Pare, D., 2000. Polarized synaptic interactions between intercalated neurons of the amygdala. J. Neurophysiol. 83, 3509–3518.
Sansig, G., et al., 2001. Increased seizure susceptibility in mice lacking metabotropic glutamate receptor 7. J. Neurosci. 21, 8734–8745.
Saugstad, J.A., Kinzie, J.M., Shinohara, M.M., Segerson, T.P., Westbrook, G.L., 1997. Cloning and expression of rat metabotropic glutamate receptor 8 reveals a distinct pharmacological profile. Mol. Pharmacol. 51, 119–125.
Shigemoto, R., Kulik, A., Roberts, J.D., Ohishi, H., Nusser, Z., Kaneko, T., Somogyi, P., 1996. Target-cell-specific concentration of a metabotropic glutamate receptor in the presynaptic active zone. Nature 381, 523–525.
Shigemoto, R., et al., 1997. Differential presynaptic localization of metabotropic glutamate receptor subtypes in the rat hippocampus. J. Neurosci. 17, 7503–7522.
Singewald, N., Sinner, C., Hetzenauer, A., Sartori, S.B., Murck, H., 2004. Magnesium-deficient diet alters depression- and anxiety-related behavior in mice – influence of desipramine and *Hypericum perforatum* extract. Neuropharmacology 47, 1189–1197.
Sreepathi, H.K., Ferraguti, F., 2012. Subpopulations of neurokinin 1 receptor-expressing neurons in the rat lateral amygdala display a differential pattern of innervation from distinct glutamatergic afferents. Neuroscience 203, 59–77.
Stachowicz, K., Klak, K., Pilc, A., Chojnacka-Wojcik, E., 2005. Lack of the antianxiety-like effect of (S)-3,4-DCPG, an mGlu8 receptor agonist, after central administration in rats. Pharmacol. Rep. 57, 856–860.
Su, H.S., Bentivoglio, M., 1990. Thalamic midline cell populations projecting to the nucleus accumbens, amygdala, and hippocampus in the rat. J. Comp. Neurol. 297, 582–593.
Swanson, C.J., Bures, M., Johnson, M.P., Linden, A.M., Monn, J.A., Schoepp, D.D., 2005. Metabotropic glutamate receptors as novel targets for anxiety and stress disorders. Nat. Rev. Drug Discov. 4, 131–144.
Tanaka, J., Nakagawa, S., Kushiya, E., Yamasaki, M., Fukaya, M., Iwanaga, T., Simon, M.I., Sakimura, K., Kano, M., Watanabe, M., 2000. Gq protein alpha subunits Galphaq and Galpha11 are localized at postsynaptic extra-junctional membrane of cerebellar Purkinje cells and hippocampal pyramidal cells. Eur. J. Neurosci. 12, 781–792.
Toth, I., Dietz, M., Peterlik, D., Huber, S.E., Fendt, M., Neumann, I.D., Flor, P.J., Slattery, D.A., 2012. Pharmacological interference with metabotropic glutamate receptor subtype 7 but not subtype 5 differentially affects within- and between-session extinction of Pavlovian conditioned fear. Neuropharmacology 62, 1619–1626.
Turner, B.H., Herkenham, M., 1991. Thalamoamygdaloid projections in the rat: a test of the amygdala's role in sensory processing. J. Comp. Neurol. 313, 295–325.
Ugolini, A., Large, C.H., Corsi, M., 2008. AMN082, an allosteric mGluR7 agonist that inhibits afferent glutamatergic transmission in rat basolateral amygdala. Neuropharmacology 55, 532–536.
Vertes, R.P., 2004. Differential projections of the infralimbic and prelimbic cortex in the rat. Synapse 51, 32–58.